EXPERIMENTS WITH HYDROCARBON BUBBLE CHAMBERS

by

A. F. McFarlane.

Department of Natural Philosophy,

University of Glasgow.

Thesis presented to the University of Glasgow,
May 1959, for the Degree of Doctor of Philosophy.

Preface

The work reported in this thesis was performed in the Department of Natural Philosophy of the University of Glasgow from September 1955 to September 1958.

In 1953 D.A. Glaser, of the University of Michigan successfully photographed trails of vapour bubbles formed by ionising particles in a liquid medium; the instrument which he invented came to be called the bubble chamber. In October 1954, in the University of Glasgow, work was initiated upon the design and development of bubble chambers for work on nuclear disintegrations produced by the photon beam of the 340 MeV synchrotron. At that time very little information had been published on the technique of bubble chamber construction.

By September 1955 I.R. Birss had constructed a small glass chamber of 4 cc. capacity similar to the type first used by Glaser and he was then joined by the author who assisted in the construction of electrical and photographic equipment associated with the operation of this chamber. Tracks were photographed in November 1955, the first successful repetition in the United Kingdom of Glaser's achievement.

The author, in collaboration with Birss, then designed and constructed further glass chambers of 20 cc. capacity.

These chambers were employed for an experimental study of the relation between the linear bubble density produced by minimum ionising particles and the operating conditions of the chamber, namely temperature and pressure. The results, obtained jointly, are described in chapters III, and IV.

Following normal nomenclature the above type of chamber, having perfectly smooth glass walls, is designated in what follows as a "clean" chamber, as opposed to the type of chamber constructed from metal with glass windows which is called a "dirty" chamber. The design and construction of a 100 cc. "dirty" chamber, requiring original development, was then undertaken by the author alone. The chamber was completely successful with fillings of both propane and isopentane. Knowledge gained from this chamber was used in designing and constructing a 500 cc. chamber in collaboration with Birss. Many tracks of electrons protons and mesons were observed; measurements of bubble density were made on these tracks under varying chamber conditions, again in collaboration.

Chapter V is the author's interpretation of the results of the bubble density investigations. It is shown that the theories of Glaser and Bertanza are inadequate to explain results obtained. The author provides an alternative theory of bubble nucleation, which is shown to agree with the available experimental

evidence and to explain many of the observed phenomena.

The author next undertook the task of construction of a large bubble chamber intended particularly to record tracks of heavy particles, primarily photomesons, produced by the direct passage of a narrow photon beam through the liquid. A propane chamber, 10" in diameter, of five litres capacity, with thin beam entry and exit windows was designed by the author and successfully put into operation. About one thousand photographs were taken and 250 heavy particle events observed. Useful information about the future application of hydrocarbon chambers to the investigation of photodisintegrations was obtained and interpreted by the author, who was assisted in the operation of the chamber by J.M. Scarr.

The work presented in this thesis was supervised by Professor P.I. Dee and Mr. J.R. Atkinson whose help is gratefully acknowledged.

The author wishes to thank Dr. W. McFarlane and the synchrotron operators for their co-operation; also Mr. J.T. Lloyd and Mr. R. Irvine for their technical services. His thanks are also due to his colleagues Mr. I.R. Birss and Mr. J.M. Scarr.

The author is indebted to the Department of Scientific and Industrial Research for a maintenance allowance during the period of this work.

Contents

Chapter I. INTRODUCTION.

The field of nuclear physics has been considerably widened in recent years by significant advances in the techniques of acceleration of particles, and in the methods of detection of nuclear events. With the availability of large fluxes of high energy particles and photons for nuclear bombardment the development of efficient particle detectors for specific purposes has become of primary importance.

It is necessary in the investigation of any process involving a nucleon- nucleon, or photon - nucleon interaction, to measure as many as possible of the properties of the initial and final particles. Ideally, accurate observation should be made of the nature, the energy and the direction of propagation of all the particles, or photons, which take part in any given reaction. The detectors used for this purpose determine some of these factors in such a way that the others may be deduced. The development of efficient detectors is an essential step towards the solution of the problems associated with the structure of the nucleus.

There are two main groups into which particle detectors may roughly be divided, namely, electronic and visual systems. Electronic systems employ one or more kinds of counter and the pulses produced by them can be analysed by the use of electronic apparatus into the required results. In most observations, by these systems, some selection has to be made by bias or coincidence methods to separate the pulses produced by the event under investigation from the pulses produced by other events.

The visual systems produce a photograph of the tracks left by ionising particles taking part in the event and therefore separation of wanted and unwanted information is simpler; however, to obtain a similar number of measurements, visual techniques generally require more time than the electronic systems. Much depends on the actual measurements which are required as to which particular detectors are most suitable for the purpose.

Until recently the visual detectors comprised the Wilson cloud chamber and the nuclear emulsion. The former, which can be the expansion type or the diffusion type, provides a gaseous medium over whose nature and density the operator has considerable control. This has meant that extensive investigations

have been possible into a great many nuclear reactions involving a range of energies from a few KeV to several MeV. Also by the introduction of metal plates into the chamber high energy cosmic ray investigations have been possible. The nuclear emulsion does not have the advantage of this control over the medium but, having a high density, is capable of providing information on the higher energy reactions, in particular those involving mesons.

There is no doubt that a detector combining some of the advantages of the cloud chamber and the nuclear emulsion would have many applications in high energy physics. Such a detector, giving a photographic record of the track of an ionising particle in a liquid medium, was first envisaged by Glaser.

Glaser considered the possibility of creating an unstable equilibrium by superheating a liquid which could be utilised in a manner similar to the supersaturation produced in a cloud chamber. By heating a volatile liquid under pressure in a smooth glass vessel and releasing the pressure, Glaser showed that boiling could be delayed until the vessel

was traversed by an energetic cosmic ray or was irradiated from a radioactive source. (ref.1). The success of this experiment led Glaser further to control the conditions and to photograph, by means of a high speed cine-camera, the development of a row of bubbles produced by the passage of a cosmic ray through the vessel. Thus in May 1953 Glaser (ref. 2) was able to report the successful observation of a particle track in a 'bubble chamber' filled with ether.

Since then the development of the bubble chamber has been extremely rapid. Other experimenters succeeded in showing that both liquid nitrogen and liquid hydrogen could be made radiation sensitive and it seems that most liquids, including liquid helium, may be used as a bubble chamber filling.

By comparing this new detector with the cloud chamber and nuclear emulsion, and by listing the advantages and disadvantages a clear idea can be formed of the potentialities of the technique. The basic property which all these have in common is that a record of all ionising tracks is made in such a way that it is possible to reconstruct the

dynamics of any reaction in three dimensions.

The range of energies over which the bubble chamber is useful is similar to that of the nuclear emulsion, perhaps even greater, as use can be made of dense liquids, such as tungsten hexafluoride and methyl iodide, covering the region from 1MeV to 100MeV. This region is complementary to the cloud chambers and can provide a valuable extension to the knowledge which has been gained on such problems as high energy nucleon - nucleon scattering and the production of mesons.

One of the chief advantages of the cloud chamber is that the filling substance may itself be used as target material for bombardment by particles or photons. This then can also be the case for the bubble chamber which may be filled with such simple nuclei as hydrogen, deuterium and helium. Nuclear emulsions necessarily contain silver and bromine -- both complex nuclei -- limiting its usefulness as a target material. With the possibility of using almost any liquid as a target, within which tracks may be photographed, the technique becomes one of the most powerful methods available for nuclear experimentation.

An important property of the bubble chamber is that the liquid medium provides a target of high cross section. Thus a filling of hydrogen becomes effectively a high density proton target. Such a dense target of elementary nuclei, in which any event can be observed from its origin, permits a fuller investigation, in the bubble chamber, of interesting low cross-section reactions.

The measurement of the energy of a particle is generally made, in the three visual detectors, by a measurement of range which can be related to energy. As in the case of the cloud chamber, magnetic fields, necessarily of higher intensities, may also be used for measurements of momentum in a bubble chamber. The use of grain density measurements in emulsions and drop density measurements in cloud chambers has its parallel in bubble density measurements for the estimation of particle velocity; this aspect is discussed fully in a later chapter.

In a comparison of cloud chambers and bubble chambers one important difference must be stressed; the ions which form droplets in a cloud chamber persist on the track for tens of milliseconds but there

is evidence to show that the latent image of a track in a bubble chamber lasts for less than a microsecond. This means that counter control of the chamber, which has been a valuable aspect of cloud chambers, is not possible in practice in the case of the bubble chamber. However, for the reason that the image is so short lived, the bubble chamber may be recycled as soon as the vapour formed has been condensed. This condensation is possible within a time of milliseconds whereas a cloud chamber takes several seconds to recover its sensitivity. This means that for experiments involving low cross-sections the bubble chamber suffers from the fact that an expansion cannot be chosen to occur when the event under investigation is detected by a counter system. The bubble chamber is capable of cycling at the pulse rate of most pulsed particle accelerators and so the photograph may be chosen as desired, by counter control of the illumination.

There is therefore little difference in the capabilities of the bubble chamber as compared with the cloud chamber and since these detectors, as regards useful regions of investigation, are complementary, it may be expected that the bubble chamber will be as important a method of particle

detection as the cloud chamber has proved to be.

Before discussing the construction and operation of some particular bubble chambers and the knowledge gained from them, it is necessary to understand the principles behind their operation.

The necessary unstable condition, namely superheat, is obtained in a bubble chamber by a reduction of the pressure on the liquid rather than an increase of the temperature. The liquid is heated above its boiling point at atmospheric pressure usually to about two thirds of its critical temperature. A pressure is applied which is just greater than the saturated vapour pressure at this temperature; thus there is no vapour present after this compression. A rapid release of this pressure, say to atmospheric pressure, leaves the liquid superheated and it will boil, on any disturbance, until the pressure increases to the saturated vapour pressure at the working temperature.

If the vessel used to contain the heated portion of the liquid is made of smooth glass there may be a delay of up to one minute between the release of the pressure and the occurence of boiling. Such a smooth-walled chamber was the type first used by Glaser.

For the measurement of angles and distances within the liquid plane glass walls are desirable; all-glass chambers with plane walls cannot withstand high pressures and are therefore limited in their application. It was thought, at first, that no superheat would be obtainable in a metal chamber with plane glass windows. The effect of the 'roughness' at the metal-glass junction or at the gaskets would be expected to initiate boiling during the release of pressure thus preventing a pressure reduction below the saturated vapour pressure. This effect is observed if any particle of dirt or roughness occurs in an all-glass chamber.

However, Wood (ref.3) and other experimenters found that if the pressure were reduced very quickly sufficient superheat could be obtained in metal chambers to make the liquid sensitive to ionising radiation. This type of chamber became known as a 'dirty' chamber and the all-glass chambers as 'clean' chambers. In fact due to their many constructional and photographic advantages bubble chambers are now mostly of the 'dirty' type.

The conditions of operation of a bubble chamber are fully determined if the temperature of the

liquid and the superheat obtained in the expansion are known. Superheat is defined as the difference between the equilibrium saturated vapour pressure, at the temperature of operation, and the pressure in the liquid when the particles enter the chamber. The particles are generally timed to coincide with the lowest pressure reached in the expansion and this pressure is referred to as the bottom pressure.

Thus the superheat δP is defined as $P_\infty - P_o$ where P_∞ (T) is the saturated vapour pressure at temperature T, and P_o is the bottom pressure.

Chapter 11. INITIAL DEVELOPMENT.

First tracks in a small 'clean' chamber.

With the object of photographing a bubble track in a super-heated liquid it was decided to build a bubble chamber of similar design to that of Hildebrand. (ref. 4).

Iso-pentane was chosen as the filling liquid since it contains only hydrogen and carbon, and, having a normal boiling point of 26°C, is a liquid at room temperatures; while the temperature of operation, about 130°C, is easily attainable. The vapour pressure at 130°C is 13 atmospheres; thus the apparatus had to be able to stand, without leak or rupture, repeated pulses of pressures of this order. The apparatus, see Fig. 1., consisted of a 4cc. glass bulb on the end of a thick walled glass tube about 20cm. long, so that the chamber was remote from the expansion apparatus. The tube was attached to the expansion apparatus, and the isopentane was separated from the moving parts by a neoprene diaphragm. An 8mm. diameter piston moved in a well filled with glycol which had an outlet to a Bourdon tube pressure gauge. This piston was connected to

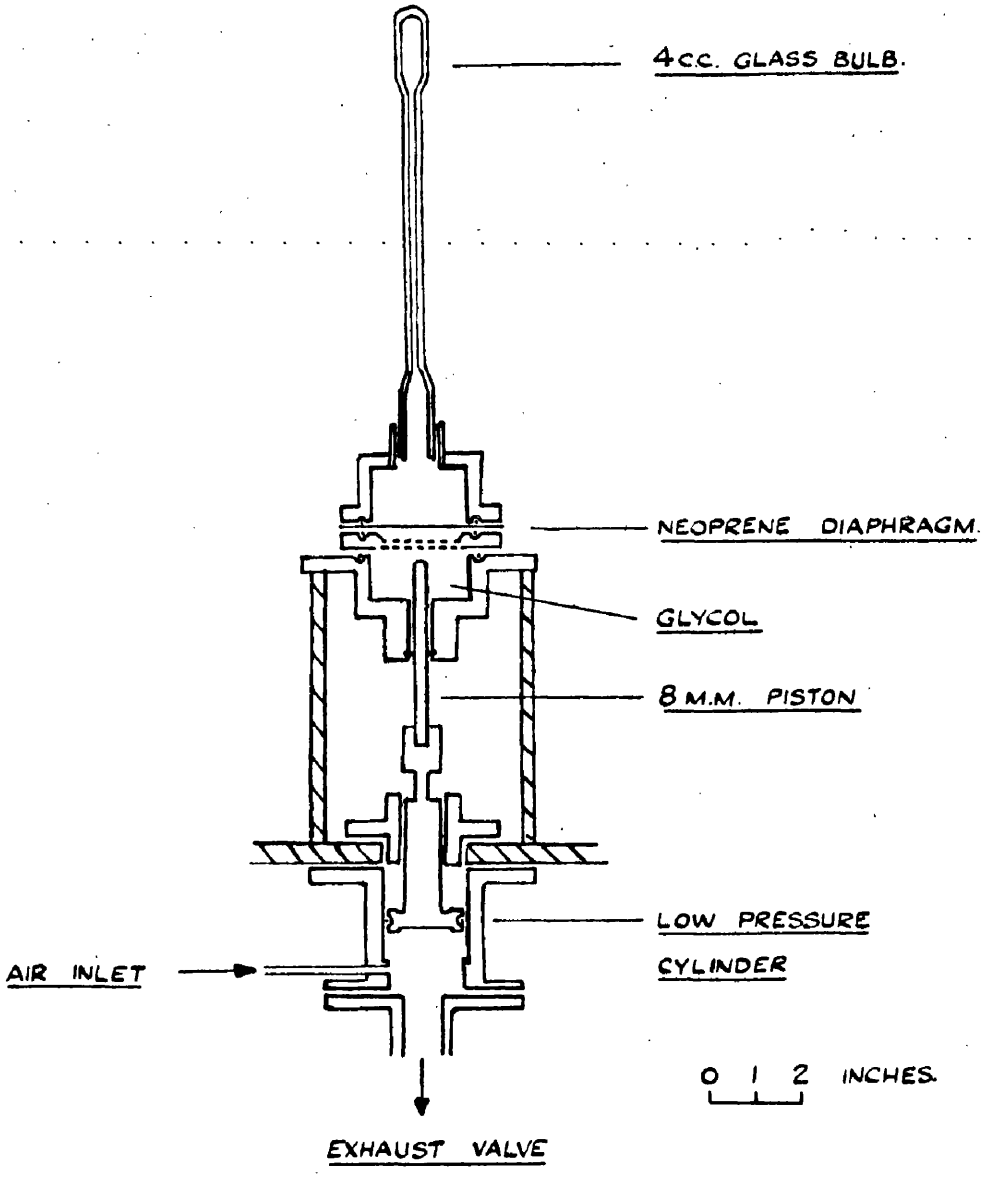

Figure 1. Diagram of the 4cc. 'clean' chamber, of a design similar to Glaser's first chamber.

a second piston of 5cm. diameter moving in a second cylinder permitting the use of low pressure air for the compression of the chamber. A magnetic valve controlled the flow of air.

The glass bulb, which was the highest point of the apparatus, was enclosed in a bath filled with glycerine which could be electrically heated to the required temperature.

Before attempting to photograph tracks with the apparatus an indication of its sensitivity was obtained by destroying the superheat, which in such a 'clean' chamber may continue for several seconds after the expansion, by irradiation from a γ-ray source or by X-rays. It was in fact found that the chamber could be made to boil in its expanded state by irradiation with X-rays of quite low energy, and that, as may be expected, smaller fluxes were required as the superheat was increased.

To obtain particle tracks in the chamber it is necessary to illuminate the chamber with a flash of short duration, soon after the particles pass through the chamber. It must therefore be possible to control accurately the instant at which illumination

occurs as bubble growth is very rapid. By charging a 1μF condenser to 5 kilovolts and discharging it across a spark gap in air, using a hydrogen filled thyratron as the triggering device, a spark of about 2 microseconds duration was obtained and the timing of this spark had less than 1 microsecond jitter.

The γ-ray beam of the 340 MeV electron synchrotron was fired into a target close to the chamber. For the first experiments the temperature of the chamber was chosen so that the chamber would remain in the sensitive state for several seconds; the beam was fired during this time by manual control. A pulse was obtained from an ionisation chamber in the γ- beam which triggered the spark about 2 microseconds after the beam.

Fig. 2 shows a photograph taken in this way. Although the intention was to observe tracks by shadow in the illuminated centre region, a track can be seen arrowed which shows up by scattered light. This track was in fact the first bubble chamber track to be photographed in Europe. The chamber temperature was 125°C and the bottom pressure one atmosphere.

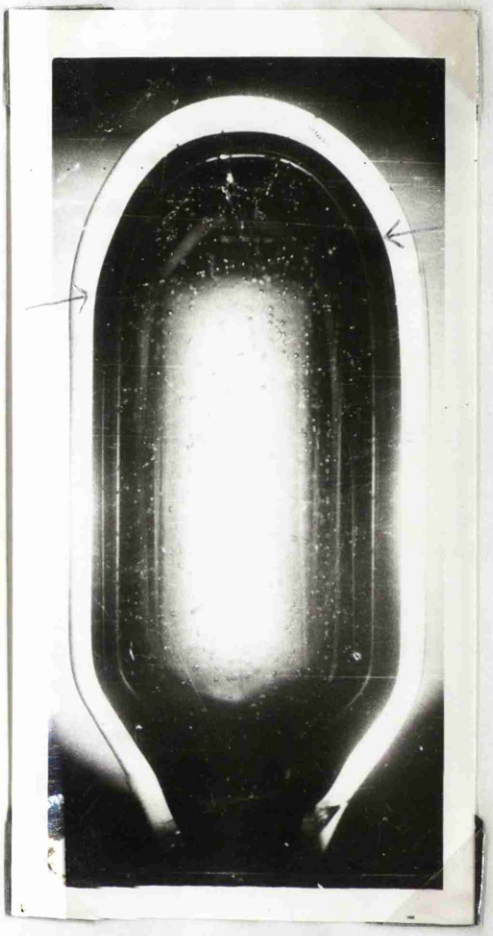

Figure 2. First tracks obtained in the 4cc. chamber. An electron track is arrowed.

Improvement of track quality.

The photographic system was obviously unsatisfactory and many different arrangements of spark and camera were subsequently tried. The shape of the chamber made uniform illumination difficult and both 'dark field' (the bubbles scattering light from a screened source into the camera) and 'bright field' (the bubbles showing dark against a bright background) were used. Finally a lens, with the spark at its focus, and a diffusing screen between the lens and the chamber, was adopted, giving bright field illumination.

To improve the track quality and to have greater control over the conditions, several modifications had to be made to the chamber.

A second piston, with a screwed movement, was introduced to permit adjustment of the pressure to which the chamber was expanded. This pressure may be measured accurately on a Bourdon tube pressure gauge since a 'clean' chamber will normally have a delay before boiling occurs. Such accurate control over the bottom pressure is an important modification.

It was decided to increase the working volume from 4 cc. to 20cc., the chamber consisting of a glass cylinder 4 cm. long and 2.5 cm. in diameter.

Although a cylindrical shape is a disadvantage in photography it was found to be necessary for strength. In fact a glass chamber of about 20cc. capacity was made with flat faces but proved to be too weak to withstand working pressures.

It was found necessary, in order to prevent chemical contamination of the pentane, to replace the neoprene diaphragm with a .015 in. thick copper-beryllium diaphragm. The chamber, with these modifications, is illustrated in fig. 3. To reduce friction in the expansion system the second piston was replaced by a cam wheel driven by an electric motor. The small piston was maintained in the compressed position, and released to effect the expansion, by a solenoid not shown in the diagram.

An electron pair spectrometer in the beam of the 340 MeV synchrotron was employed to provide a beam of approximately monoenergetic electrons of 100 MeV at an angle of 30° to the beam. The 20cc. clean bubble chamber was situated so that this beam of minimum ionising electrons would pass through the chamber. The beam of the synchrotron was timed, by a switch on the expansion mechanism, to come within

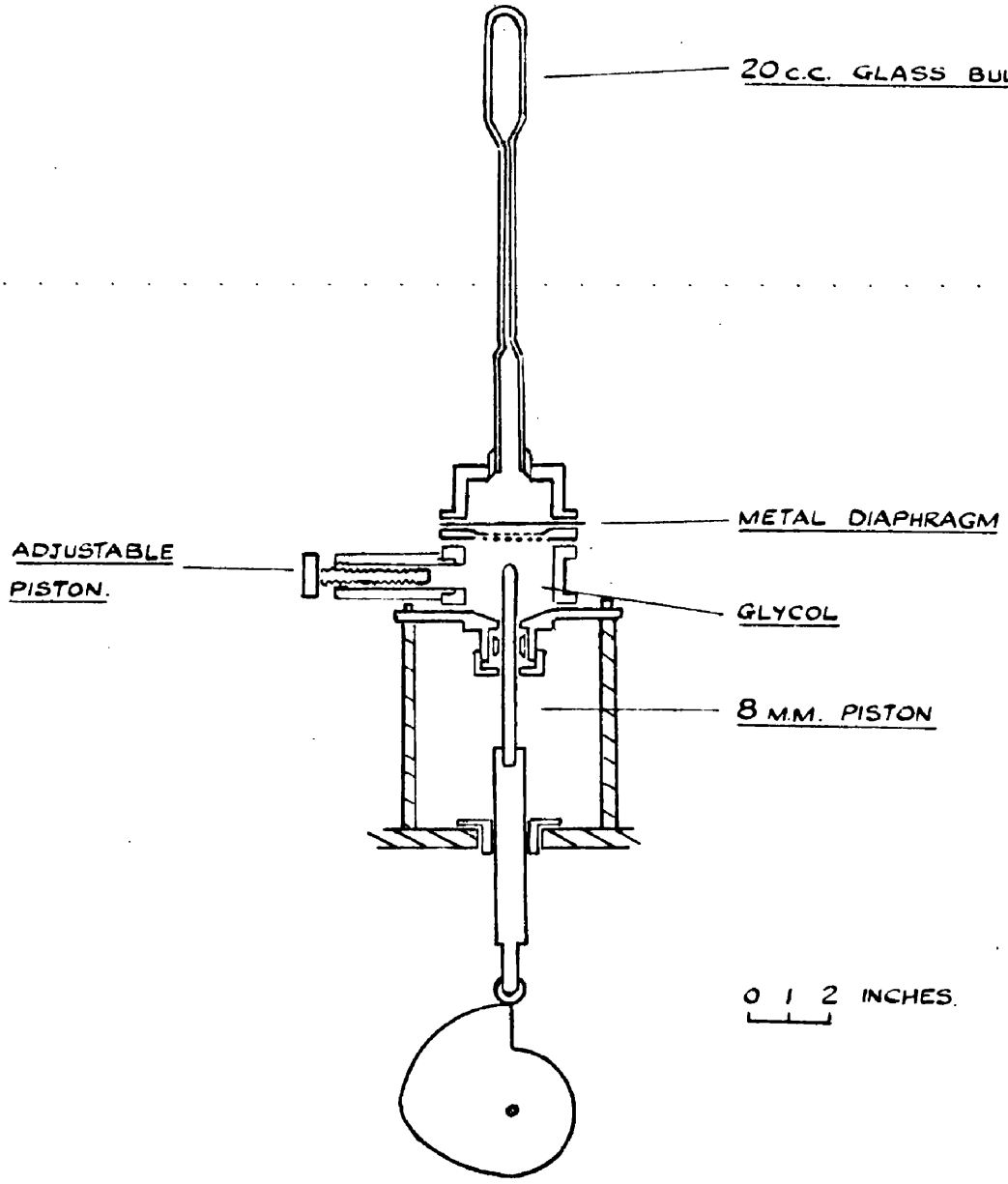

Figure 3. Diagram of the 20cc. 'clean' chamber in which the effect of conditions of operation on bubble density was studied.

$\frac{1}{4}$ second of the expansion. The spark illumination was triggered from scintillation counters in the positron beam of the spectrometer, with a variable delay between the beam pulse and the spark.

Both chamber temperature and spark delay were varied. At 128°C with a delay of 4 microseconds between beam and spark no bubbles were seen, but with a delay of 35 microseconds bubbles were just visible. The next photographs were taken at 134°C and 500 microseconds delay and fairly good tracks were observed (fig. 4). The chamber was gradually cooled again and as the temperature decreased the number of bubbles per centimetre observed on the tracks also decreased; no bubbles were formed below 126°C. A decision to change to bright field illumination improved the appearance of the tracks as shown in fig. 5 taken when the chamber temperature was 136°C and the spark delay 40 microseconds.

Thus the primary object of photographing bubble chamber tracks of ionising particles was attained.

Figure 4. Early tracks in the 20cc. chamber using 'dark field' illumination.

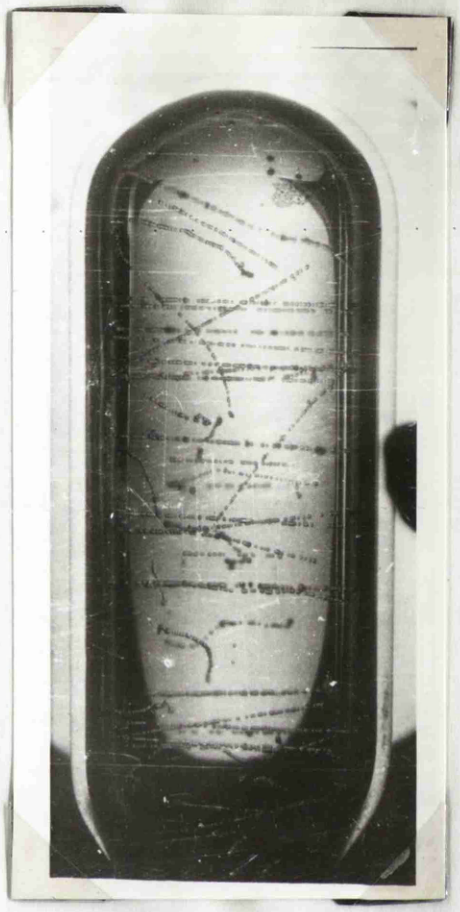

Figure 5. Electron tracks in the 20cc. chamber using 'bright field' illumination.

Chapter III. BUBBLE DENSITY ON PARTICLE TRACKS.

Variables affecting track bubble density.

It was clear from these experiments that the number of bubbles observed and the clarity of the tracks were dependent on many factors. Pressure and temperature both affected track quality in no obviously predictable manner and it was felt that a closer study would be valuable. Certainly if the bubble chamber is to be efficiently applied it is necessary to know the optimum conditions of operation and to know in what manner a variation of these parameters would affect the formation of tracks. If also it proves to be desirable to measure the energy of a particle, or more probably, to identify a particle, by the nature of its track, a fuller understanding must be gained of the behaviour of the chamber under different conditions.

The final appearance of a recorded track depends therefore, to a greater or lesser extent, on the following variables — working liquid, temperature of operation, bottom pressure, time of illumination and the velocity, mass and charge of the ionising particle.

It was decided, therefore, to carry out a

detailed investigation of the effect of these variables on bubbles density i.e. number of bubbles per unit length of track. The investigation to be carried out in two parts; the first being the investigation of the effect of chamber conditions on the tracks of identical particles, namely minimum ionising electrons, and the second relating the bubble density, under constant chamber conditions, to the nature of the particle .

Variation of bubble density with chamber conditions.

Since it was possible to measure accurately the necessary variables affecting the chamber in the 20cc 'clean' chamber described above, this chamber, with further modifications, was suitable for the first part of the investigation.

A more satisfactory system for triggering electronically the expansion of the chamber was designed, this was necessary since at the high temperatures required for electron sensitivity the average 'delay' time is only a few milliseconds. However it was still possible to measure the lowest pressure reached during expansion. The most convenient source of homogeneous particles, necesary for the investigation of the effect of varying chamber

conditions on particle tracks, was avilable from the pair spectrometer and again 100 MeV electrons were chosen.

Keeping the bottom pressure constant at one atmosphere and varying the temperature of operation, several hundred photographs similar to fig. 5 were taken. An analysis of these photographs was made by reprojection and by microscope study of the negatives.

The results are shown in fig. 6 which is a graph of the bubble density along tracks of 100 MeV electrons as a function of temperature in an iso-pentane filled chamber expanded to one atmosphere. A discussion of the results is left to a later chapter.

With the same experimental arrangement several hundred more photographs were taken with different values of bottom pressure; in this case the temperature was maintained at a constant value. This experiment was performed for two values of the temperature, namely 133°C and 136°C and the results are shown in fig.7 which is a graph of track bubble density versus superheat. Although Glaser has published (ref.5) a graph of temperature dependence similar to fig. 6 for π-meson tracks in propane the bottom pressure in his

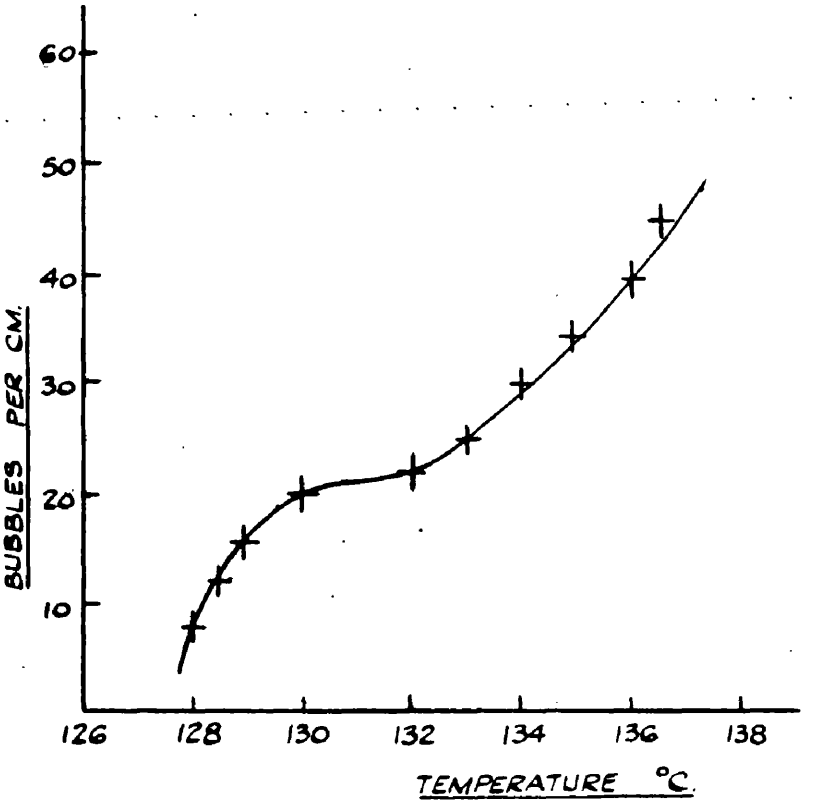

Figure 6. The temperature dependence of bubble density on tracks of 100 MeV electrons. The chamber liquid was iso-pentane and the expanded pressure 1 atmosphere.

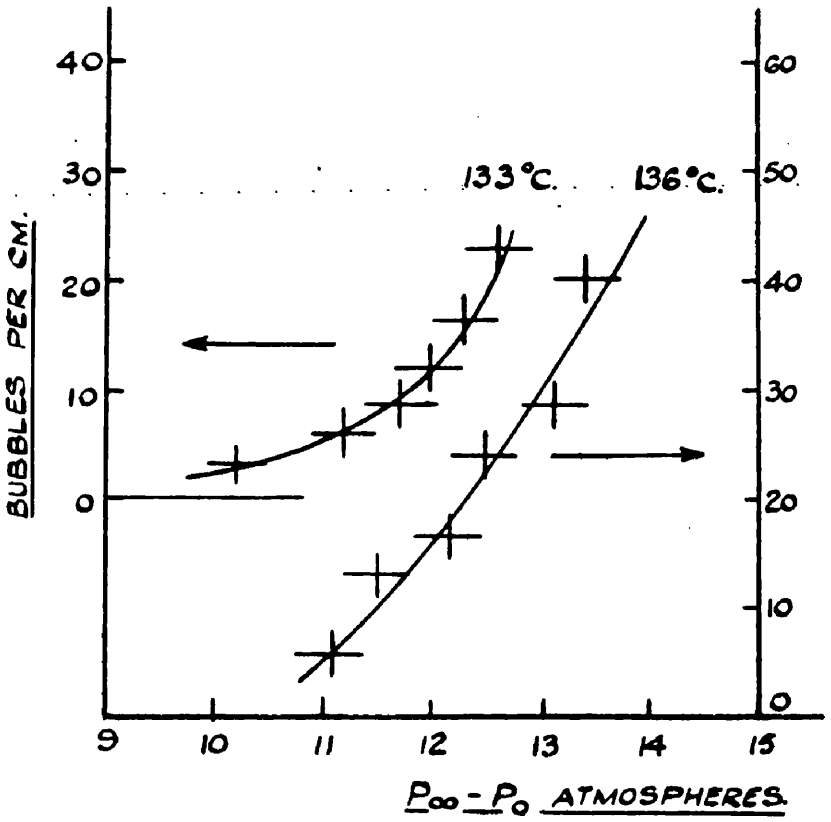

Figure 7. Bubble density as a function of superheat. Measurements were made on tracks of 100 MeV electrons in iso-pentane.

chamber was not known. Also Blinov (ref.6) has published a result for the dependence on bottom pressure in propane which corresponds closely in shape to the curves of fig. 7, but only gives his temperature of operation within a few centigrade degrees.

These results, for other particles in propane, do not overlap the results of figs. 6 and 7 but it is significant that the curves given byboth Glaser and Blinov correspond closely in their characteristics to those obtained in the isopentane chamber.

Variation of bubble density with nature of particle.

The second, and perhaps more important, part of the investigation of the factors controlling the nature of a track is concerned with the effect of the particle itself on the bubble density observed along its track.

If the process of bubble formation were an ionisation process then it might be expected that the number of bubbles per cm. would be proportional to the ionisation — unless some masking or coalescence affects the results for high densities. Again if the number of bubbles observed is small, with gaps

in the track up to .5cm long, as is quite usual, then it would be difficult to account for this on an average ionisation theory. In the case of the cloud chamber each ion may produce a droplet and in emulsions each grain ionised is developable. This means that the number of droplets or grains is of the same order as the number of ions formed. Although bubble chamber tracks can be observed with as many as 100 bubbles per cm. or as few as one bubble per cm. the ionisation is of the order of 10^6 ion pairs per cm. which is several orders of magnitude larger. This means that there may not be any direct proportionality between bubbles and ions.

From the appearance of many tracks, however, it is obvious that as a particle slows down, and is more heavily ionising, more bubbles are produced. Thus bubble formation depends, directly or indirectly, on energy loss by the particle.

Particle identification and velocity measurement.

For the purpose of this investigation it is required to indentify particles (electron, proton or meson) and to make measurements at various points on the tracks.

The most reliable method of determining the nature of the particle concerned is to observe the nature of its ending, if it comes to rest in the chamber. An electron, for instance, if not minimum ionising, suffers multiple scattering and is easily identifiable if it stops. In fact the range of a slowing electron does not allow measurements of bubble density on any part of the track where the relativistic velocity ratio β differs appreciably from unity. A proton of less than 20 MeV will not, in general, react with the medium and will suffer little scattering whereas a π^+- meson will most probably decay into a μ^+-meson and subsequently to an electron. A π^--meson has a high probability of reacting with a nucleus, especially in a hydrocarbon chamber, ejecting one or more nucleons which may be observed in the chamber.

Since it is necessary for identification to observe the particle stopping in the chamber, a convenient method of measuring its velocity at any point on the track is by calculation from the known range/energy relations. Everything that is required may therefore be determined if the particle is stopped in the chamber. The volume of the chamber thus

becomes of great importance as it must be possible to observe a reasonable length of track and to stop a reasonable number of particles in the chamber.

The size and shape of the 'clean' chambers described above make them unsuitable for this application. Because of the limits imposed on the volume of a clean chamber by the strength of the glass attempts had been made, by Glaser and others, to construct bubble chambers from metal cylinders with glass windows. The difficulties introduced in obtaining sufficient superheat in spite of the discontinuities involved at the glass and metal junctions had largely been solved by more efficient methods of expansion. An increase in the temperature of operation, compared with 'clean' chambers, was also necessary to compensate for the reduction in superheat caused by immediate boiling in these so called 'dirty' chambers.

It was decided, therefore, that there would be many advantages in relinquishing the clean chambers and further developing the technique by the construction of one or more 'dirty' chambers; this development being primarily for application to the above investigation.

Chapter IV. DEVELOPMENT OF LARGER CHAMBERS.

Design of a 100cc. 'dirty' chamber.

In the construction of this type of chamber many new experimental problems are introduced. It is not easy to seal the chamber, at the glass metal junction, under conditions of high temperatures and high pressures and still present as little roughness to the working liquid as possible. As a gasket material no type of rubber is suitable as the action of pentane, or propane, will destroy the rubber or be itself contaminated by soluble products in the rubber. However, polished fluon gaskets have been found to be satisfactory in most respects. The expansion appartus chosen for the 'dirty' chambers does not differ appreciably from the 'clean' chamber apparatus except that a more rapid expansion is obtained by improvements in the detailed design.

Fig. 8 is a diagram of a 100cc. chamber which was constructed to investigate the special properties of a 'dirty' chamber and to complete the investigation of the effect of the nature of the particle on track density. It consisted of a brass cylinder 2in. deep

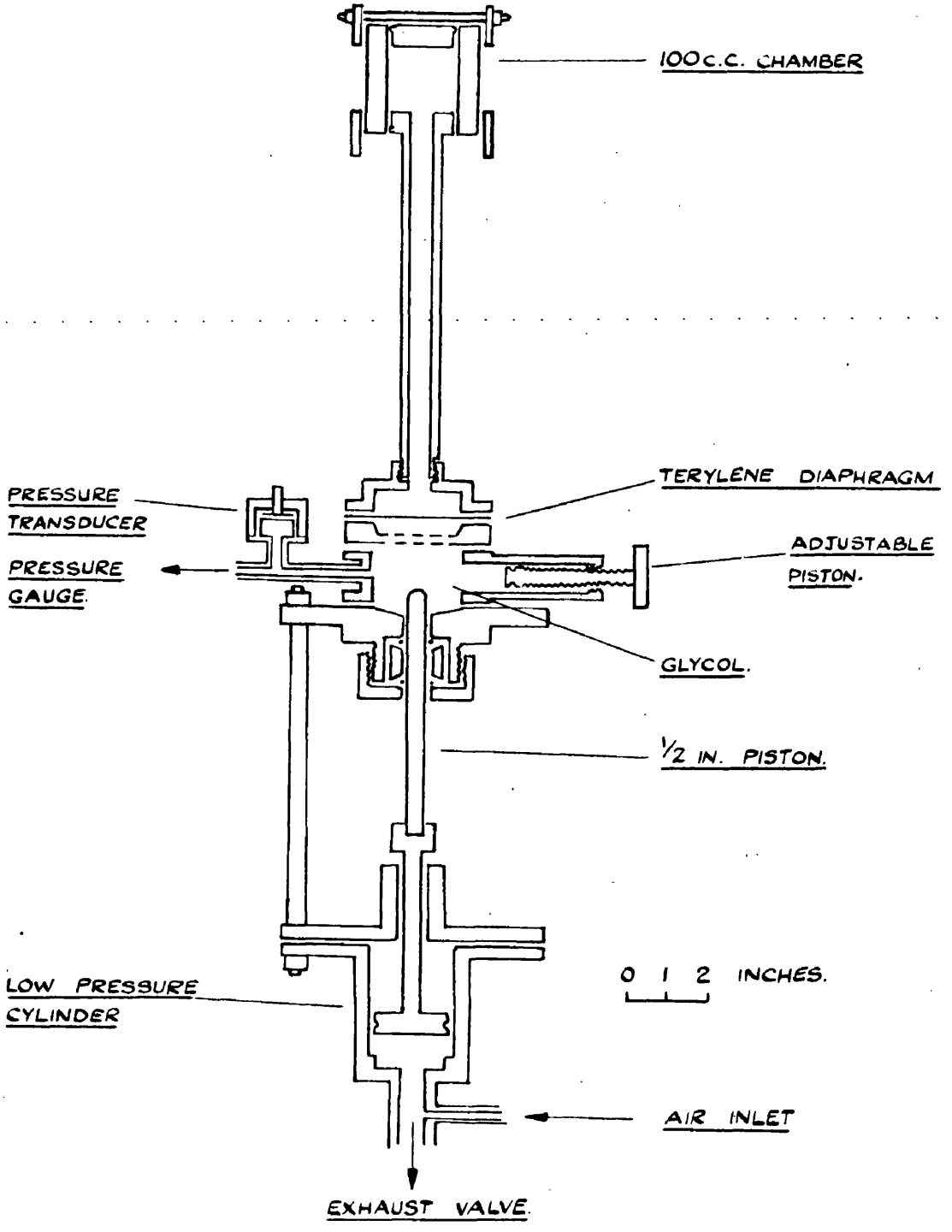

Figure 8. Diagram of the 100cc. 'dirty' chamber which was used for preliminary measurements relating bubble density and particle velocity.

and 2 in. in diameter with $\frac{1}{2}$ in. thick glass windows. The filling liquid, propane or pentane, was separated by a terylene foil diaphragm, from the glycol in which a $\frac{1}{2}$ in. diameter piston moved to effect the compression and expansion. This piston is connected to a larger piston in a low pressure cylinder. An improved gland for the $\frac{1}{2}$ in. piston and a modified exhaust valve allow a more rapid expansion to be made.

Since the sensitive time of a 'dirty' chamber is very small compared with the delay time of a 'clean' chamber, it is necessary to have exact control over the moment at which particles enter the chamber. The short sensitive time is a result of the immediate boiling which occurs on the walls and at corners in a 'dirty' chamber. Such boiling tends to destroy the superheat and opposes the action of the expansion.

By comparing the pressure change in both types of chamber, shown diagrammatically in figs. 9(a) and (b), it is seen that the 'dirty' chamber cycle (b) is on a much shorter time scale and the immediate boiling prevents the pressure falling to a low value. The position of the beam of particles, in time, must occur for the 'dirty' chamber at or near the point of

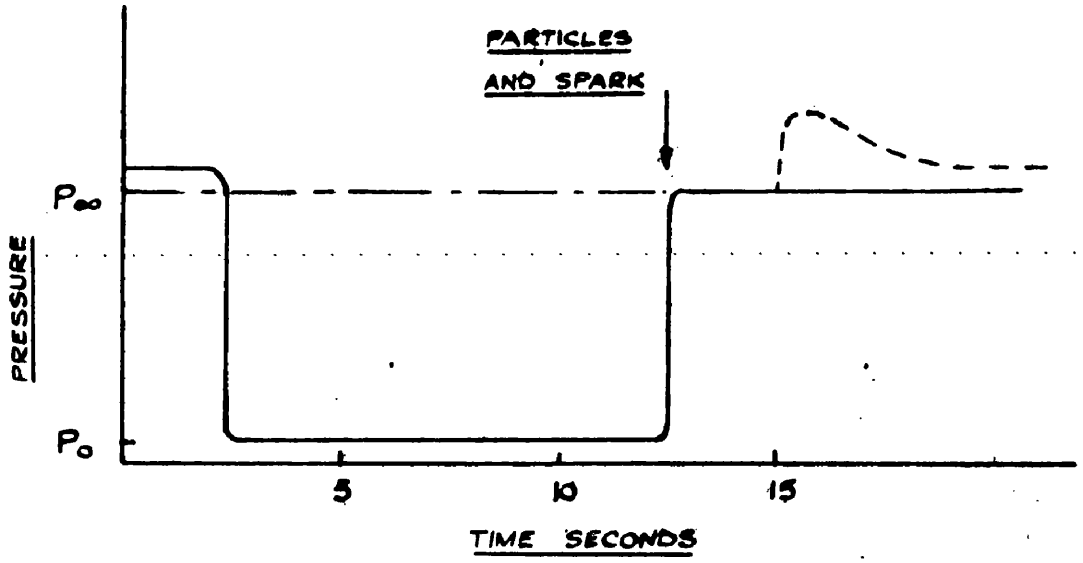

Figure 9 (a). 'Clean' chamber pressure cycle.

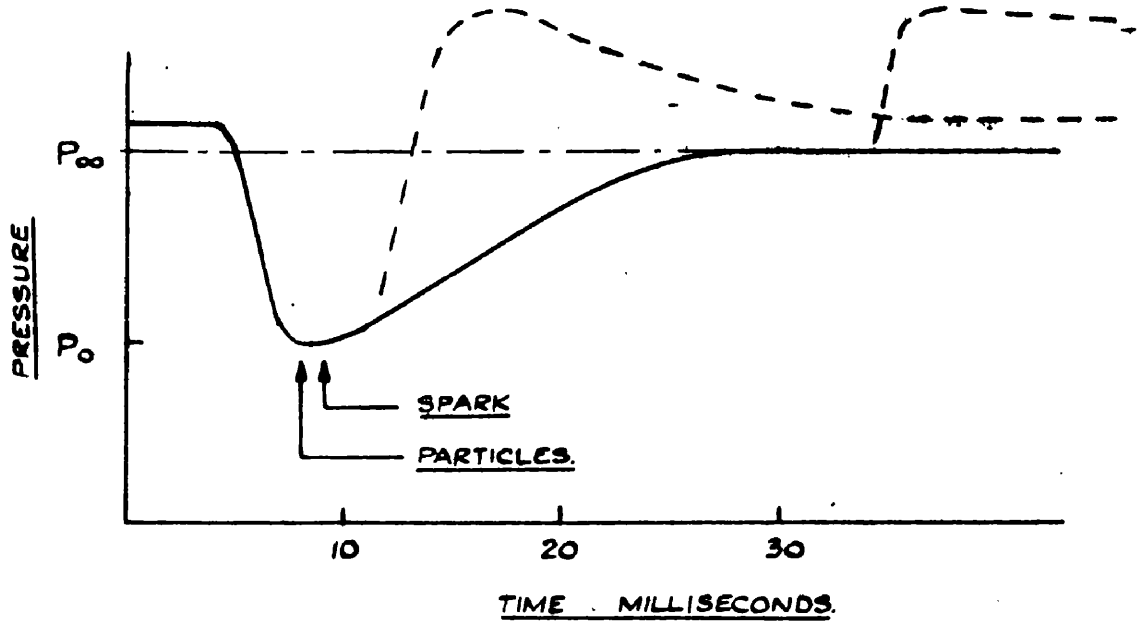

Figure 9 (b). 'Dirty' chamber pressure cycle.

maximum superheat, and the illumination about a millisecond later.

In the clean chamber the particles themselves cause the boiling and so may occur at any time after the expansion, limited only by the probability of a cosmic ray passing through the chamber. The illumination in this case must be within a few microseconds of the particles as bubble growth is rapid in 'clean' chambers. The reason for the differences in growth rate is that the pressure in 'clean' chambers is initially considerably lower than in 'dirty' chambers presenting less resistance to the expansion of the bubbles during the early stages of their growth.

The dotted curves of fig. 9 show possible pressure changes during recompression. If the earlier one of fig. 9 (b) could be achieved by a recompression closely following the expansion less vapour would have to be condensed and the cycle would be completed earlier.

Delay units were built so that the expansion and spark could be varied at will with respect to the beam of particles. A positive indication of the sensitive time of the chamber was clearly necessary.

A pressure transducer was therefore designed which would convert the pressure pulse within the chamber to a voltage pulse which could be displayed on an oscilloscope. The transducer consists of a thin diaphragm in contact with the working liquid in the chamber. A plane disc of insulated brass is adjusted to be close to this diaphragm. Change in pressure therefore registers as a change in capacity of this system. This change in capacity is converted to a voltage change by using the capacity to control the frequency of an oscillator and detecting the frequency modulation. Although this does not give a linear response it proved to be capable of a reasonable approximation.

Fig.10 is a double beam oscilloscope trace of a typical sequence of events in the 100 cc. chamber. The time base is triggered by the pulse which cuts off the magnetic valve current. The pressure begins to drop after 70 milliseconds, reaching its lowest value 7 milliseconds later and the chamber is sensitive for a few milliseconds after that. The oscillation which occurs at 90 milliseconds is due to a shock wave set up when the piston reaches the bottom of its travel. The lower oscilloscope trace

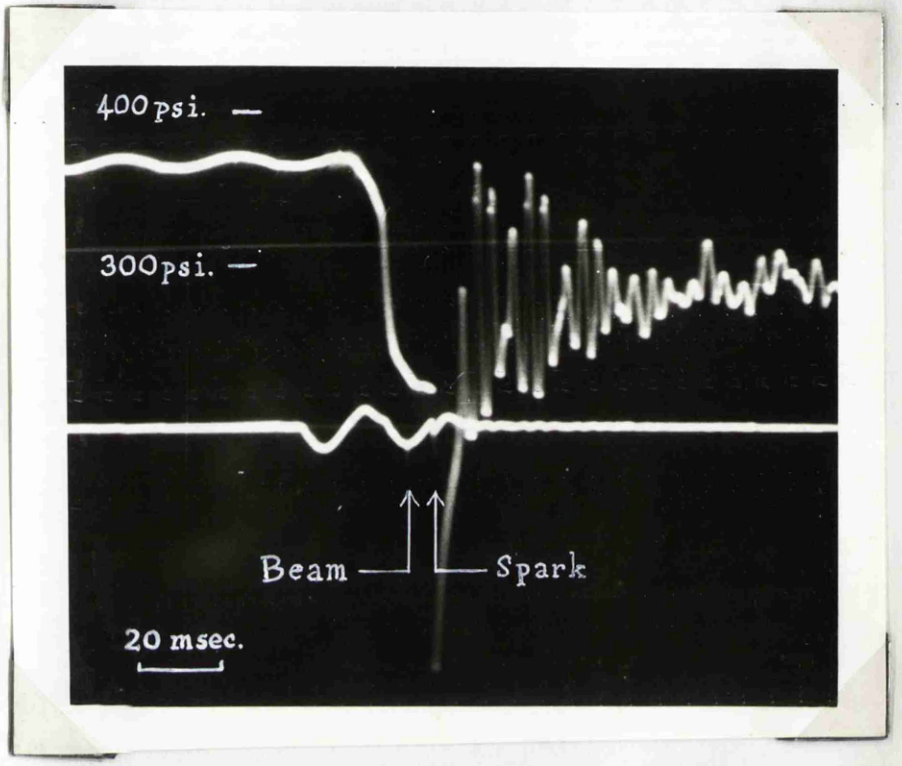

Figure 10. Oscilloscope trace of the pressure pulse in the 100cc. chamber. The lower trace indicates the timing of the synchrotron beam and the spark illumination.

shows the beam pulse; the spark shows up by radio frequency pick-up on both traces. Fig.11 shows a photograph of electron tracks corresponding to this timing, taken during the testing of the chamber. It appeared that the sensitive time of the chamber, i.e. the time during which the beam could occur producing visible tracks, lasted for about 8 milliseconds.

Effect of operating conditions on tracks in the 100 cc. Chamber.

Although the main objective at this time was to investigate the effect on bubble density of the nature of the particle it was felt that it would be valuable, in conjunction with the necessary testing experiments for the new chamber, to repeat the bubble density verus temperature measurements.

With the 'dirty' chambers it was only possible to estimate roughly the bottom pressure attained during expansion, as the transducer does not give an accurate reading. However the temperature variation of the bubble density on electron tracks in isopentane is plotted in fig. 12 for an estimated bottom pressure of 8 atmospheres. Although this

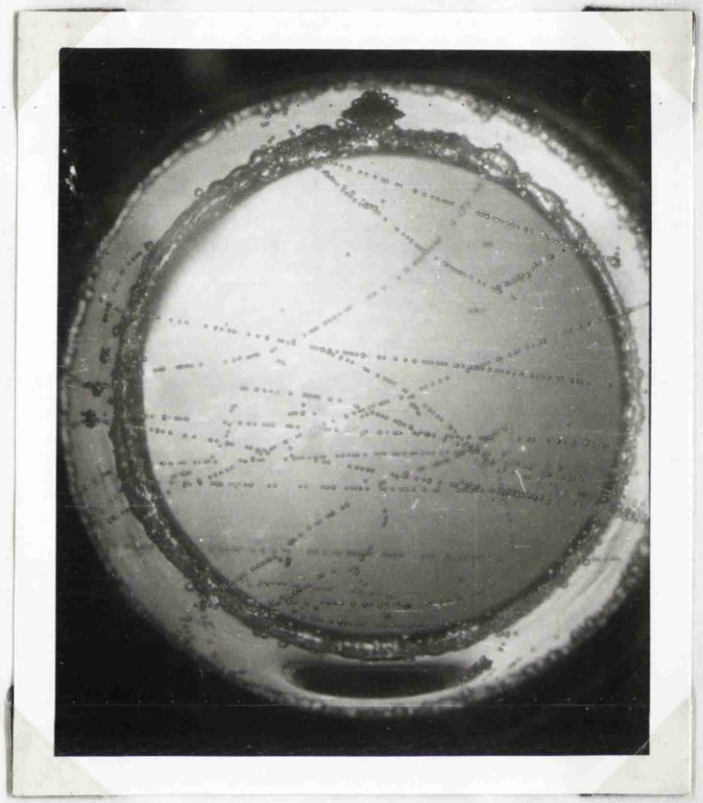

Figure 11. Electron tracks in the 100cc.'dirty' chamber.

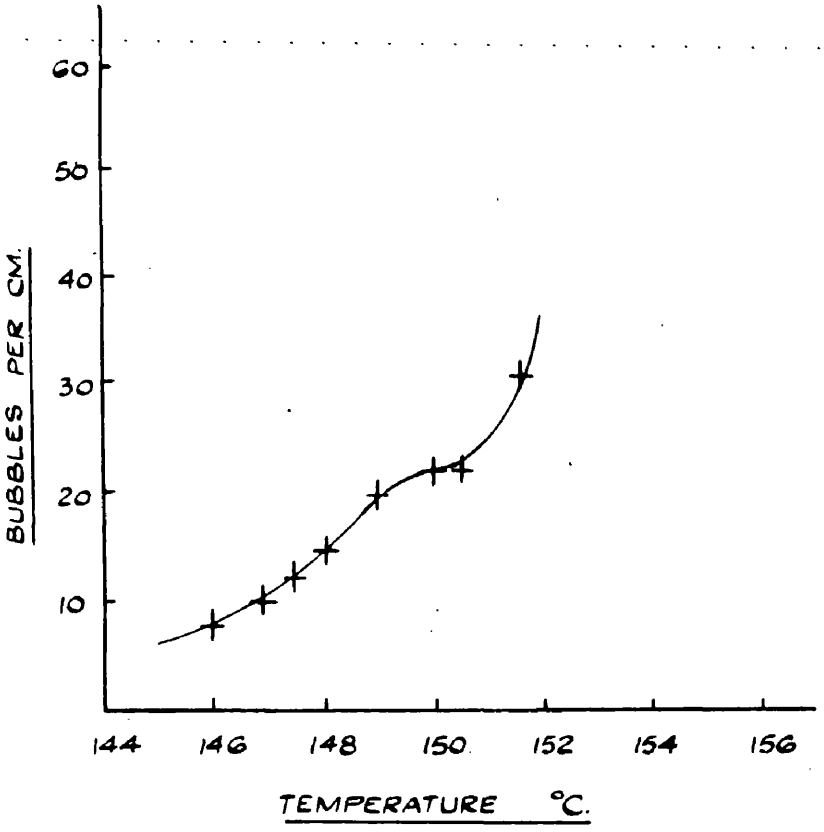

Figure 12. The temperature dependence of bubble density on tracks of 100 MeV electrons in a 'dirty' chamber filled with iso-pentane. The expanded pressure was not accurately known.

value is quite different from the 1 atmosphere obtained in the 'clean' chambers the graphs of bubble density as a function of temperature show a remarkable similarity of shape although covering a different temperature range.

Another change that was made at this time was to alter the filling liquid from isopentane (C_5H_{12}) to propane (C_3H_8) which proved to be more convenient for chamber operation. Again bubble density in propane was investigated as a function of temperature, for electrons, during the testing of the chamber (see fig. 13). This cannot be compared directly with Glaser's results (ref.5) for minimum ionising π^- mesons, which is also shown on fig. 13, as in neither experiment was the bottom pressure accurately known, although both have indications of the characteristic 'plateau' which tends to appear in all such graphs. This is important as it shows that the 'plateau' effect is not particular to one filling substance but is more probably connected with the fundamental process of the formation of bubbles on the tracks of ionising particles.

Returning to the problem of relating bubble density to the nature of the particle it is required

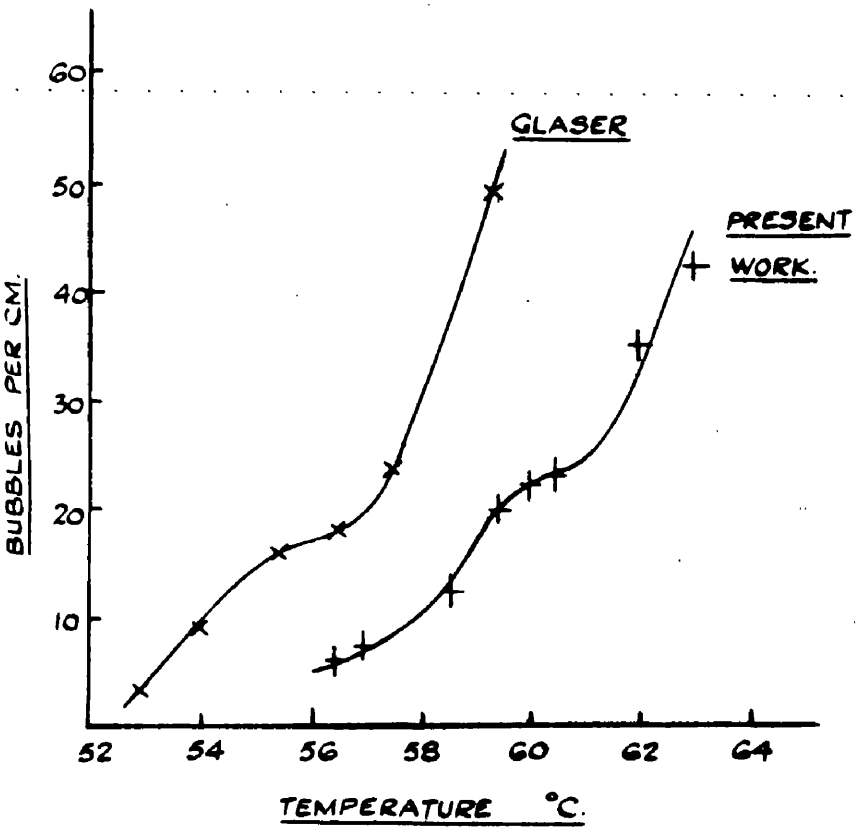

Figure 13. The temperature dependence of bubble density on tracks of 100 MeV electrons in the propane filled 100 cc. chamber, and on tracks of minimum ionising pions in Glaser's propane chamber. In neither case was the expanded pressure known; Glaser evidently obtained a greater degree of superheat.

to photograph tracks of mesons and protons stopping in the chamber. Such mesons and protons are produced, together with many electron pairs, when the photon beam of the 340 MeV synchrotron strikes a solid target of any material. If the bubble chamber is positioned at a backward angle to the direction of the beam the ratio of heavy particle to electrons is higher than in the forward direction. Using a carbon target of about 10 gm/cm^2 a few cm from the chamber and a beam of 10^6 equivalent quanta per pulse the bubble chamber detects two or three heavy particles per photograph. Photographs similar to that of fig. 14, which shows a proton stopping in the chamber, were taken with the 100 cc. chamber.

Design of a 500 cc. chamber.

Only a limited number of measurements could however be made with sufficient accuracy in this chamber and a further chamber of 500 cc. volume was built (fig. 15).

As an alternative to a piston system of expansion a diaphragm which allows a more rapid expansion was preferred. The chamber is compressed and expanded by changing air pressure, separated from the propane by a flexible diaphragm, from above the saturated vapour pressure to atmospheric pressure.

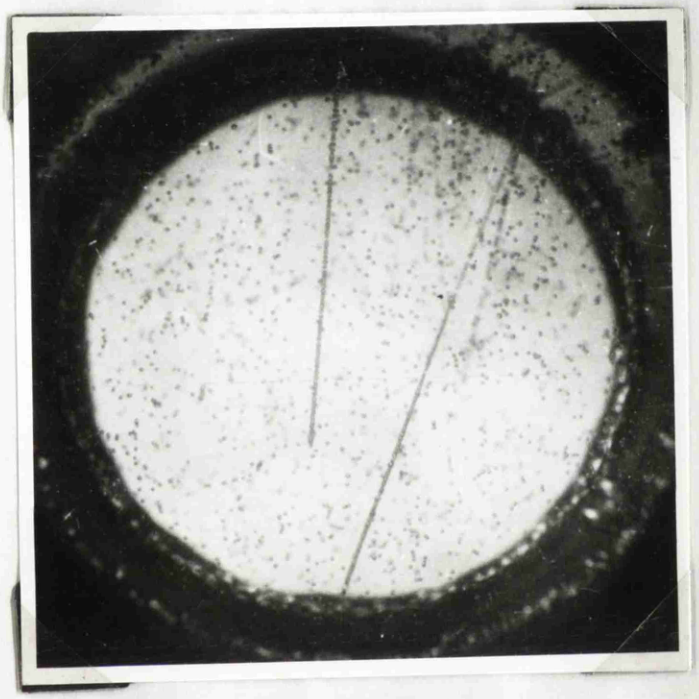

Figure 14. Proton tracks in the 100cc. chamber, one stopping.

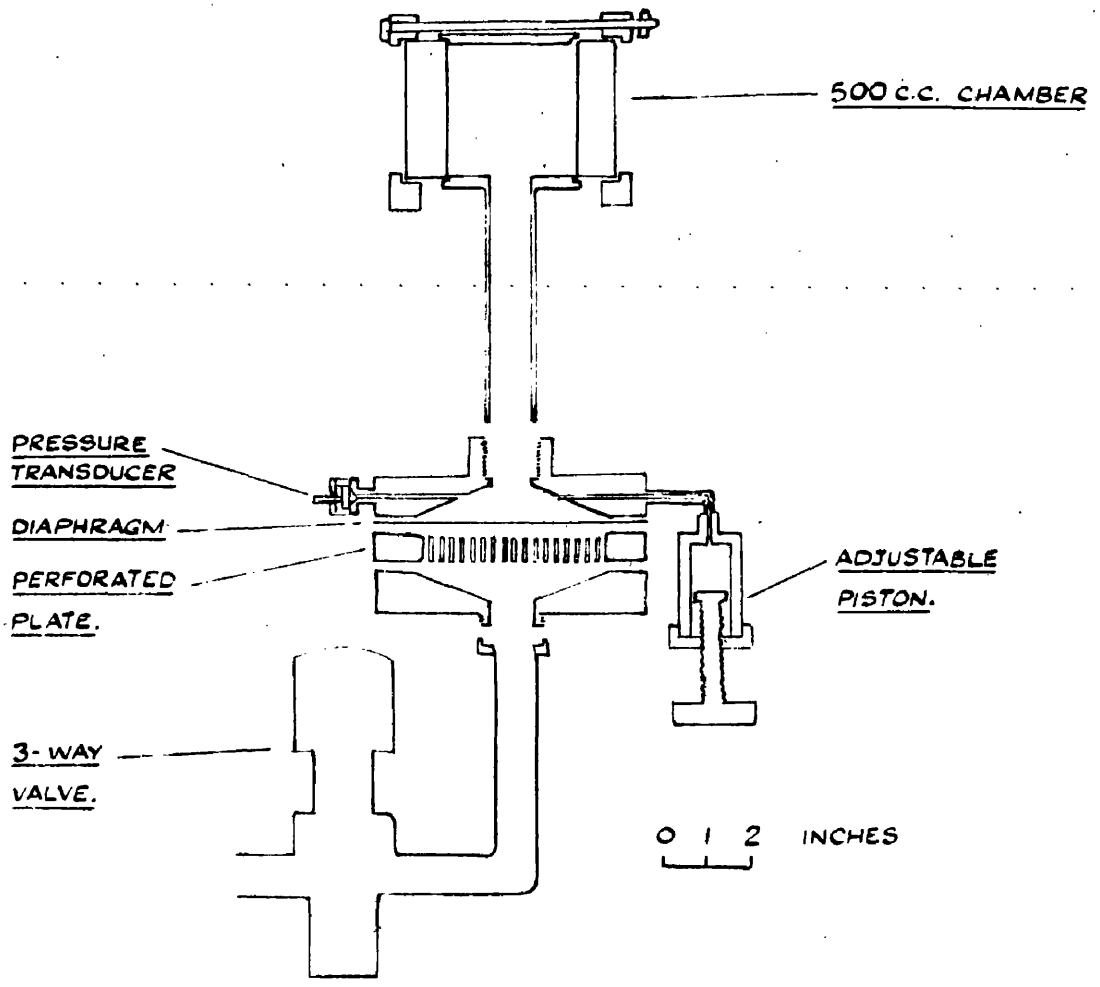

Figure 15. Diagram of the 500cc. 'dirty' chamber, illustrating the use of a direct diaphragm expansion system.

This is a pressure defined system as opposed to the volume defined (piston) systems used previously. Unfortunately no greater control over the bottom pressure results from this system as the wall boiling competes with the diaphragm movement affecting the internal pressure.

Bubble density as a function of particle velocity.

With this chamber, of greater volume, it was possible to extend the measurements of bubble density as a function of particle velocity. Bubble density as measured in the experiments, is plotted against $1/\beta^2$ in fig. 16. The linear dependence agrees with results obtained by Glaser (ref. 5) and Blinov (ref.6).

Conclusions from experiment.

Summing up, therefore, both temperature and pressure considerably affect the bubble density on a track. Bubbles first appear at a definite temperature which depends on the bottom pressure while the density ranges from zero to a hundred bubbles per cm over only a few centigrade degrees. There is evidence of a 'plateau' or at least a point of inflexion in the temperature dependence which for minimum ionising electrons always occurs at a bubble density close to 20 bubbles /cm. independently of the pressure. The effects occur for both the hydrocarbon

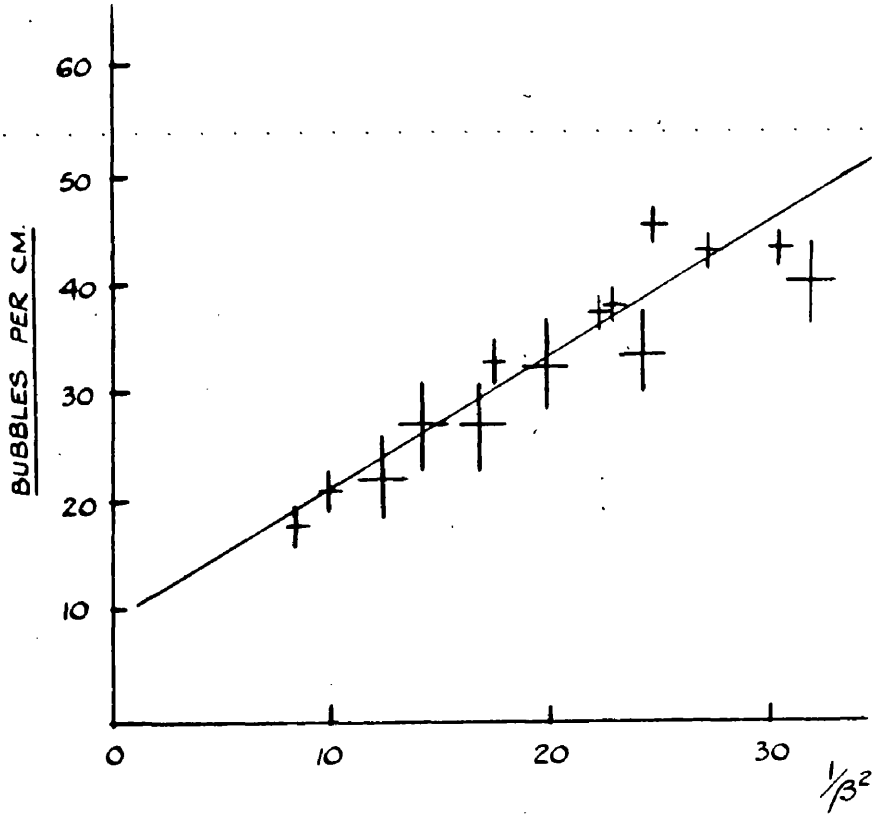

Figure 16. Bubble density as a function of particle velocity (β = velocity/c). Measurements were made on proton tracks in propane at 59.5 °C.

filling substances used, namely isopentane and propane.

The relation between temperature, superheat ($P_\infty - P_0$) and bubble density is such that an increase of the average temperature of operation can compensate for a decrease of superheat, leaving the bubble density and its characteristic dependence on small temperature variations (over less than ten centigrade degrees) unaltered. As for the ionisation of the particle as a controlling factor, it is generally found that bubble density proportional to $1/\beta^2$ describes the relation within experimental error.

The results, and their consistency, at least in character, among chambers, filling substance and experimenters, have led to an interest in the fundamental processes controlling bubble formation. The following chapter discusses the problem of bubble nucleation specifically for the clarification of the above results and for the fuller understanding that is necessary before confidently using the technique.

Chapter V. BUBBLE DENSITY THEORY.

The Problem.

The necessity of investigating the nucleation process is related to the direct application of bubble counting to determine the nature and energy of the particle causing the track. This method of identifying a particle and calculating its energy has its equivalent in drop counting on cloud chamber photographs, and grain counting on nuclear emulsions.

In the case of the cloud chamber, ionisation is proportional to the number of droplets formed and these may be counted if chamber conditions are suitable; again the blackening of nuclear emulsions is essentially an ionisation process and can be related to the energy of the particle. However the situation is different for bubble chambers where the conditions of operation play the main part in controlling the number of bubbles observed, and there is no simple relationship between the ionisation and the number of bubbles formed.

The problem has interested most bubble chamber experimenters and various experiments which help towards a solution have been performed. No

satisfactory theory has yet been published.

Theory of Glaser.

The following discussion, due to Glaser (ref. 7), attributes the growth of a bubble to electronic charges on the surface of an already formed bubble which would collapse in their absence. For an uncharged bubble which is mechanically stable, the equilibrium condition is

$$P\infty - Po = \frac{2\sigma}{r} \quad (1)$$

where $P\infty$ (T) is the saturated vapour pressure at temperature T (this is the pressure inside the bubble), Po is the outside pressure in the liquid, σ (T) is the surface tension and r is the radius of the bubble.

Glaser has shown that a single charge will cause such a bubble to collapse whereas two or more will tend to make it grow. I f the mutual repulsion of n electronic charges is treated as a pressure term adding to the pressure inside the bubble, equation (1) becomes

$$P\infty - Po + \frac{n^2 e^2}{8\pi \varepsilon r^4} = \frac{2\sigma}{r} \quad (2)$$

where ε(T) is the dielectric constant and e is the electronic charge.

For a given n, (2) gives a value of r for which $P_\infty - P_o$ is a maximum.

If the actual pressure difference exceeds the maximum then there is no value of r for which the equilibrium condition (2) holds and therefore such an n-charged bubble will grow spontaneously; that is if

$$P_\infty - P_o \geq \tfrac{3}{2}\left(\frac{4\pi}{n^2 e^2}\right)^{1/3} \sigma^{4/3} \epsilon^{1/3} \qquad (3)$$

It is difficult to connect this condition with the number of bubbles observed. From experimental values of the successful operating conditions necessary for the detection of minimum ionising particles the value of n, necessary to satisfy (3) is of the order of 6, and the corresponding radius given by equation (2) is 50 Ångstroms. This means, roughly, that 6 ions of the same sign must be found in 50 Å of track length before a bubble forms. The average energy loss by ionisation of a minimum ionising electron, say, is about 1 MeV/gm/cm.^{2} or one ion per 1000 Å in liquid propane. The probability of 6 ions being formed in 50 Å is too small to explain the observed bubble density. Glaser was led to consider the production of delta rays by the primary particle as a mechanism whereby a sufficient number of ions is produced in a small region.

When an electron is freed in the ionisation process it may be given sufficient energy to cause further ionisations, and in such a case the density of ions close to the primary track will be much greater than the average value. The number of delta rays of energy between E_1 and E_2 electron volts produced per centimetre by a particle of charge ze and relativistic velocity ratio β in a medium of density ρ and atomic and mass numbers Z, A is given by

$$1{\cdot}53 \times 10^5 \rho \frac{Z}{A} \frac{z^2}{\beta^2} \left(\frac{1}{E_2} - \frac{1}{E_1} \right) \qquad (4)$$

If, as would be reasonable to assume, delta rays of energies between certain fixed values were responsible for the production of bubbles on the track, then the number of bubbles per centimetre would be proportional to $1/\beta^2$.

Comments on Glasers Theory.

Glaser looked for such a relationship in his results but found rather that bubble density d was described by

$$d = \frac{A}{\beta^2} + B \qquad (5)$$

where A and B are constants with A independent of temperature. The only other comparable results of Blinov et al. (ref. 6) and the results of measurements on protons and mesons in the 100 cc.

and 500 cc. chambers (Chapter IV) indicate that the dependence on $1/\beta^2$ is more closely followed than Glaser found. However, a later publication by Rahm (ref. 8) who recounted Glaser's tracks and revised his values of bubble density, contradicts the earlier results and provides agreement with $d \propto 1/\beta^2$.

This would indicate, then, that the delta ray postulate was close to solving the problem. As Rahm points out (ref. 8) the average energy loss due to ionisation (inclusive of delta ray production), excitation and elastic nuclear scattering, is proportional to $1/\beta^{1.83}$ which is experimentally indistinguishable from a $1/\beta^2$ bubble density dependence.

Experiments show that the variation of bubble density with temperature has a characteristic shape independent of the nature of the liquids, bottom pressures, P_o, and particles used. There is always the suggestion of a plateau which is most definite in the clean isopentane chamber result (fig.12). If bubbles were attributable to delta rays only, a continuous variation with the temperature would be expected. Also there is no obvious explanation of

the very rapid rise of bubble density above this plateau. It is possible that two processes are operating in the formation of bubbles. The formation of bubbles by the energy released by delta rays may be supplemented at higher sensitivities by random concentration of the energy deposited along the track by excitation and recombination of single ions. The dependence on β of such a statistical distribution would be approximately of the form $B/\beta^2 e^{-C\beta^4}$ where B and C are temperature and pressure dependent terms. This means that, together with the delta ray contribution, bubble density may be written

$$d = \frac{A}{\beta^2} + \frac{B}{\beta^2} e^{-C\beta^4} \qquad (6)$$

where A also would be a function of temperature and pressure. Before the terms A, B and C can be calculated it is necessary to have a better understanding of the mechanism whereby energy can initiate a bubble in a superheated liquid. It would be expected that the values of B and C would be such that the statistical term which has come to be called the 'core' term, would be negligible at temperatures below the plateau and A would increase only slowly with

temperature. The available results, which show that bubble density is proportional to $1/\beta^2$, are taken under conditions corresponding to temperatures close to the plateau temperature where only the delta rays are expected to contribute. The variation with β of bubble density above the plateau temperature is difficult to obtain as even minimum ionising particles have high bubble densities which may be unmeasureable owing to the limited resolution of the photographic syatem.

Theory of Bertanza et al.

Bertanza et al. (ref. 9) attempt to take the step from the formation of ions to the formation of bubbles in a paper published in April 1957. It is based, in part, on Glaser's original theory of electronic charges on a bubble. The condition (equation (3)) for the spontaneous growth of a bubble containing n charges is

$$P \propto - Po \geq 3/2\left(\frac{4\pi}{n^2e^2}\right)^{1/3} \sigma^{4/3}\, \varepsilon^{1/3} \qquad (3)$$

if N_o is the first integral value of n which satisfies this inequality then $N_o + 1$, $N_o + 2$, etc. will also satisfy it. All that is required therefore is that $N_o + k$ ions whould be present in a sphere radius r_k where r_k is the value of r which corresponds to the turning value given by the equality in equation

(3), that is r_k is given by

$$r_k = \sqrt[3]{\frac{(N_o+k)^2 e^2}{4\pi\varepsilon\sigma}} \qquad (7)$$

Thus if $N_o + k$ ions are deposited in the last $2r_k$ of a delta ray track a bubble will form. Since the last part of the track is the most heavily ionising it is necessary to consider only whether or not a bubble is formed on the last part of the track. Delta rays which form more than one bubble will be apparent on the track and only one bubble will be counted.

Let E_k be the energy of the delta ray which will form $N_o + k$ ions, then if there is a probability π_k of there being $N_o + k$ ions in the last $2r_k$ of the track there is the same probability for every delta ray of energy greater than E_k. The probability can be evaluated if the mean number of ions $\bar{N}_k$ formed in the last $2r_k$ of a delta ray track is known, then

$$\pi_k = \frac{\bar{N}_k^{N_o+k} e^{-\bar{N}_k}}{(N_o+k)!} \qquad (8)$$

Thus, if for example, a delta ray has energy E_2 it has a probability of forming a bubble under the conditions necessary for $N_o + 2$ ions in $2r_2$, and for N_o+1 in $2r_1$ as well as for N_o in $2r_o$. The probability of one of these happening is

$$\pi_o + \pi_1 + \pi_2 - 2\pi_o\pi_1 - 2\pi_1\pi_2 - 2\pi_2\pi_o + 3\pi_o\pi_1\pi_2$$

Thus summing all the probabilities for k = 0,1,2,3,....

the number of bubbles due to delta rays is

$$\sum_{k=0}^{\infty} \int_{E_k}^{E_{k+1}} \left(\sum_{p=0}^{k} \pi_p - 2 \sum_{p,q=0}^{k} \pi_p \pi_q + 3 \sum_{p,q,r=0}^{k} \pi_p \pi_q \pi_r - \ldots \right) dN \quad (9)$$

where $p<q<r \ldots$, and $dN = \text{const.}/E^2 dE$ is the number of delta rays between the energies E and E + dE.

This equation gives qualitatively the hoped for dependence on temperature at temperatures below the plateau, and is practically a constant above it. Bertanza was led to postulate a further contribution from the 'core' of the track. Instead of using the charge theory of Glaser the 'core' contribution was calculated on random concentration of the energy deposited along the track. If T_k is the energy required to form a bubble radius r_k then the probability of an energy transfer greater than T_k occurring in $2r_k$ is

$$\frac{2}{\sqrt{\pi}} \int_{T_k/2\sqrt{2}\, r_k \bar{E}}^{\infty} e^{-t^2} \, dt$$

where $\bar{E}$ is the mean energy loss per centimetre of the primary particle. The value of k may be taken as zero as the contribution for k = 0 is much larger than for k=1,2,... Thus the number of bubbles due to this process is

$$\frac{1}{r_o \sqrt{\pi}} \int_{T_o/2\sqrt{2}\, r_o \bar{E}}^{\infty} e^{-t^2} \, dt \quad (10)$$

This is the statistical dependence which, if $\bar{E}$

is proportional to $1/\beta^2$, approximates to a term of the form $B/\beta^2 e^{-C\beta^4}$.

Comments on Bertanza's theory.

When the above theory is fitted to the results of Chapter III the agreement is not good. The delta ray contribution is a poor fit to the isopentane result (the only result where the bottom pressure P_o is known with sufficient accuracy) and the 'core' contribution rises too rapidly with increase of temperature.

The conditions of operation of a bubble chamber lie within close limits of temperature and pressure; at a given expansion a range of a few centigrade degrees is sufficient to take the number of bubbles per centimetre on a given particle track from zero to over 100. Thus a check can be made on the charge dependence theory of Glaser, on which Bertanza's theory is based, which indicates that for different liquids the quantity $\sigma^{4/3}(T)\,\varepsilon^{1/3}(T)/(P_\infty - P_o)$ at operating values should be approximately constant. This was in fact found by Glaser, within experimental error (ref.10). However if alpha particles were used to initiate the boiling in such experiments Glaser

found that, to agree with the theory, an alpha particle would have to deposit 900 charges of the same sign in a region 2 x 10^{-6} centimetres in diameter, i.e. the operating conditions for the detection of alpha particles were such that n in equation (3) would have to be of the order of 900. Such a high ionisation is not attained by a stopping alpha particle, even if the charge separation were possible, and so the theory is contradicted.

Proposed Theory.

In view of the failure of the theory which depends on the presence of free ions on the surface of the bubble the fate of the energy transferred to the liquid by ionisation must be considered. In a time of the order of 10^{-9} seconds most of the energy of ionisation is converted by de-excitation and molecular collision to kinetic energy of the molecules. This local heating constitutes a thermal 'spike' which may contain sufficient energy in a sufficiently small region to produce a bubble. The energy necessary to form a vapour bubble in a liquid is the sum of the heat required to lift the molecules from the liquid to the vapour phase,

together with the surface energy of the bubble and, if the pressure of the liquid is not negligible, a term representing the work done in creating the cavity in the liquid.

Thus the energy required to form a bubble radius r in the liquid is given by

$$E = \frac{P_\infty (\frac{4}{3}\pi r^3) L}{kT} + 4\pi r^2 \sigma + \frac{4}{3}\pi r^3 P_o \qquad (11)$$

where P_∞ is the saturated vapour pressure, σ is the surface tension and L is the molecular heat of the liquid at temperature T, and P_o is the pressure in the liquid (ref.11). It is assumed that the rate of growth of the bubble is so rapid and the thermal conductivity of the liquid is such that the latent heat of vaporisation is not supplied by the ambient temperature of the liquid.

The radius of a mechanically stable bubble in the liquid under the above conditions is given by

$$r_c = \frac{2\sigma}{P_\infty - P_o} \qquad (12)$$

If a bubble is formed in the liquid of radius less than the critical radius r_c the forces of surface tension will collapse it whereas a bubble of radius greater than r_c will grow until the external conditions change. With r_c substituted in equation

(11) the energy E_c is the minimum energy which is required to form a microscopic bubble which will subsequently grow to visible size. The only possible source of the dense ionisation necessary to deposit the energy required in a small region would be on the tracks of low energy delta rays produced by the primary particle.

E_c is the mimimum energy required to form a bubble but in practice the initiating delta ray will have to have a much larger energy. Most of the energy will in fact be converted into the heat energy of a thermal spike, but much of this energy will be dissipated by conduction before the growth of the bubble. An analysis of this effect has been attempted by Seitz (ref. 12) who finds that the energy required is as much as 10 to 50 times greater than E_c. No accurate analysis has been made owing to the complexity of the problem and the lack of accurate information regarding the physical quantities involved in the calculations.

If a factor α is assumed ($\alpha \sim 10$) the number of bubbles observed, for particular conditions, should be equal to the number of delta rays produced by the primary particle with energies in excess of αE_c where E_c is calculable from the conditions of

temperature and pressure in the chamber. The following formula, see equation (4), derived from Rutherford's scattering formula, is valid in the region of delta ray energies considered and gives the number of delta rays, per unit track length, having energies between E and E +dE as

$$dn_\delta = 1{\cdot}53\times10^5 \frac{\rho Z z^2}{A\beta^2} \frac{dE}{E^2} \qquad (13)$$

Thus the number of delta rays of energy greater than αE_c, and hence the number of bubbles observed, is given by

$$d = n_\delta(\alpha E_c) = 1{\cdot}53\times10^5 \frac{\rho Z z^2}{A\beta^2} \frac{1}{\alpha E_c} \text{ per cm} \qquad (14)$$

No upper limit to the energy of these delta rays need be considered as the number of delta rays which have sufficient energy to form a bubble which is definitely off the track, and therefore not counted, is small enough to be neglected.

The only experimental results available when both temperature and pressure are simultaneously known, hence enabling the calculation of E_c, are the results obtained in the clean isopentane chamber mentioned in Chapter III. Fig. 17 shows the bubble density given by equation (14)(broken

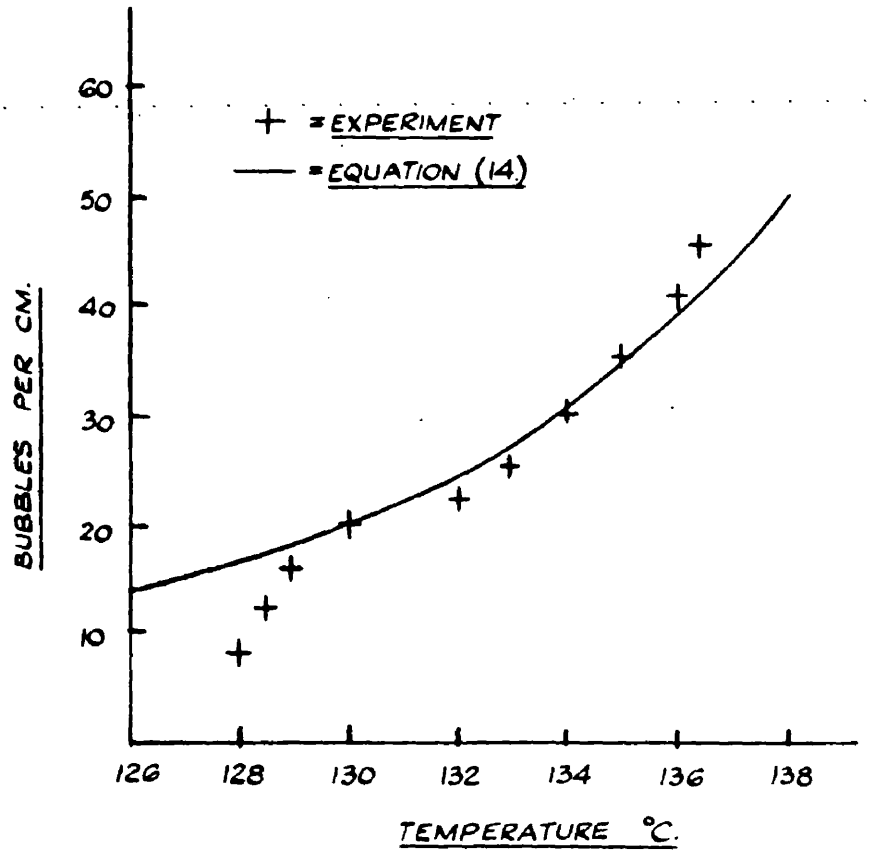

Figure 17. Equation (14) fitted to the temperature dependence of bubble density (fig. 6).

line) on the bubble density versus temperature graph with a value of $\alpha = 15.7$.

It is seen that there is a cut-off of the bubbles observed which is not indicated by the above theory. It is evident that this cut-off occurs in other results (e.g. figs. 12,13, Glaser fig.13, and Bassi's result (ref.13) in n-pentane) and is an important effect which produces a plateau in the temperature sensitivity of the chamber. It was observed from the approximate results available that this cut-off occurs at the same value of r_c (equation (12))for all the propane results.

Nothing has been said about the range of the delta ray of energy αE_c which initiates a bubble. It is obvious that if a delta ray of energy αE_c deposits sufficient energy in such a manner as to cause a bubble to form, then so also will any delta ray of energy greater than αE_c, as maximum energy loss occurs in the last part of the delta ray path. The only condition which may reasonably be required of a delta ray of energy $\geqslant \alpha E_c$ is that the part of its track corresponding to energy αE_c should have a range less than $2r_c$ and so confine its energy to the

volume of the bubble.

For delta rays of energy less than 5 KeV there is little experimental information on their practical range. If the accepted proportionality to the square of the initial energy is extrapolated to these energies a range of only a few molecular diameters is obtained. It would be unreasonable to assume, when the range is of the order of the mean free path, that the accepted formula holds.

Another unknown factor will have to be introduced to link the range and energy for such low energy delta rays. For the moment the mean range $\bar{R}$ of a delta ray of energy E will be written as

$$\bar{R} = f\ (N,Z,E) \qquad (15)$$

where N is the number of molecules per cc. of the liquid and Z is the number of electrons per molecule.

This range will suffer a statistical straggling, similar to that suffered by alpha particles in passing through an absorber, and will result in a gaussian distribution of width perhaps a few percent of the average range. If this range is of the order of $2r_c$ then a cut-off would occur when the range of the delta ray of energy $\propto E_c$,

which is a function of the temperature and the expanded pressure of the liquid, P_o, exceeded $2r_c$ and would not therefore be confined to a sufficiently small volume. Thus, to a first approximation, no bubbles would be formed at temperatures and pressures such that

$$2r_c(T,P_o) < \bar{R}_c\ (T,P_o) \qquad (16)$$

where $\bar{R}_c$ is given by $E = \alpha E_c$ substituted in equation (15).

The chamber conditions corresponding to $2r_c = \bar{R}_c$ effectively consitute a threshold of sensitivity which will occur at a certain value of $\bar{R}_c$ (and of r_c) say $\bar{R}_c^x$. Both of the functions $2r_c$ and $\bar{R}_c$ decrease with increasing temperature and superheat, but for values of these conditions lower than the threshold $\bar{R}_c > 2r_c > \bar{R}_c^x$ and for higher values $\bar{R}_c < 2r_c < \bar{R}_c^x$, and of course at the threshold value $\bar{R}_c = 2r_c = \bar{R}_c^x$. If the range of the delta ray of energy αE_c is in fact accurately described by a gaussian distribution about the mean value $\bar{R}_c$ then this threshold is not an absolute barrier.

The following cases arise;

I. $\bar{R}_c \ll 2r_c \ll \bar{R}_c^x$ (see fig. 18).

The gaussian curve indicates the distribution of the range of the last part of the track (which deposits energy αE_c) of the delta-rays of energy $\geqslant \alpha E_c$. In this case the mean range $\bar{R}_c$ of delta-rays of energy αE_c (which corresponds to the conditions defining r_c) is much less than $2r_c$ and all delta-rays of energy $\geqslant \alpha E_c$ will create bubbles at the end of their path.

Thus number of bubbles formed $= n_\delta(\alpha E_c)$. See equation (14).

II. $\bar{R}_c \gg 2r_c \gg \bar{R}_c^x$ (fig. 19).

In this case the mean range $\bar{R}_c$ of delta-rays of energy αE_c is much greater than $2r_c$ and no delta-rays of any energy will create bubbles.

III. $\bar{R}_c \simeq 2r_c \simeq \bar{R}_c^x$ (fig. 20 (a), (b) and (c)).

In this case the mean range $\bar{R}_c$ of delta-rays of energy αE_c lies close to $2r_c$. The number of bubbles which will be formed is equal to the number of delta-rays which deposit energy αE_c within the distance $2r_c$.

Thus number of bubbles $= n_\delta(\alpha E_c) \times \frac{1}{\sqrt{\pi}} \int_{-\infty}^{x} e^{-\frac{1}{2}t^2} dt$

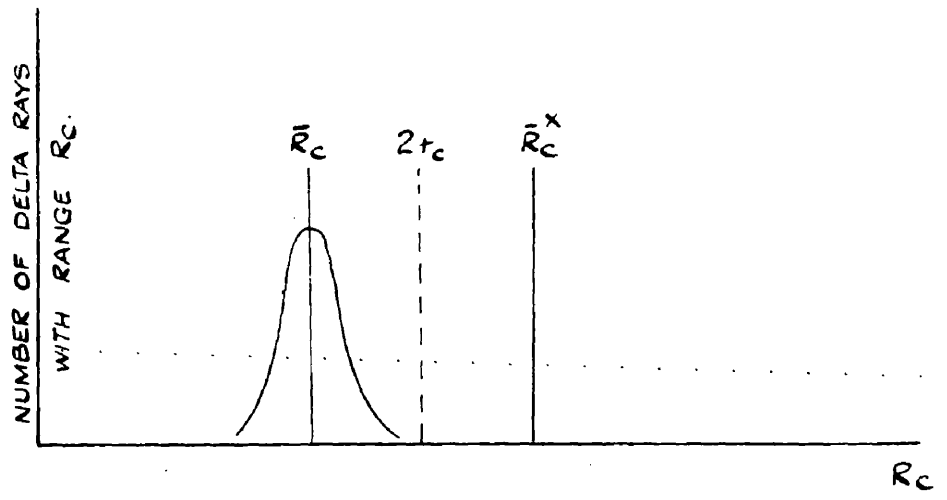

Figure 18. Case I. $\bar{R}_c \ll 2r_c \ll \bar{R}_c^x$. The gaussian curve illustrates the distribution of effective delta-ray ranges, R_c, about the mean $\bar{R}_c$.

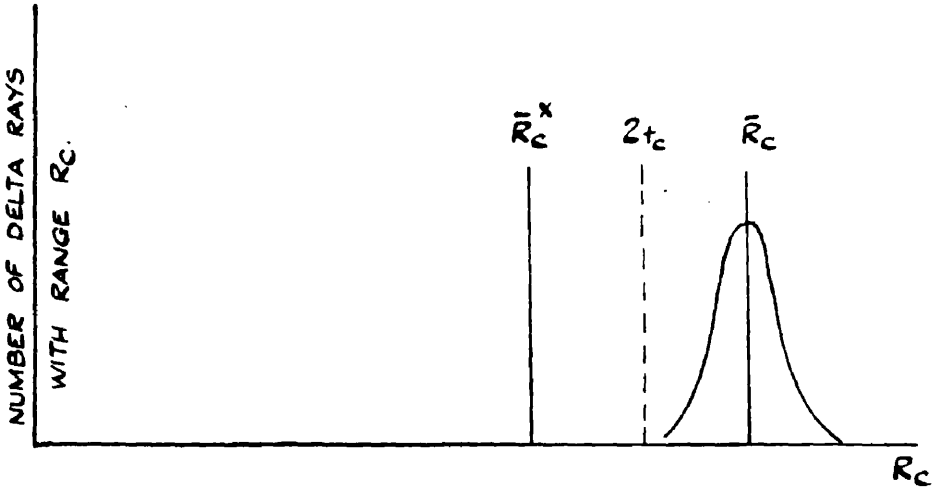

Figure 19. Case II. $\bar{R}_c \gg 2r_c \gg \bar{R}_c^x$.

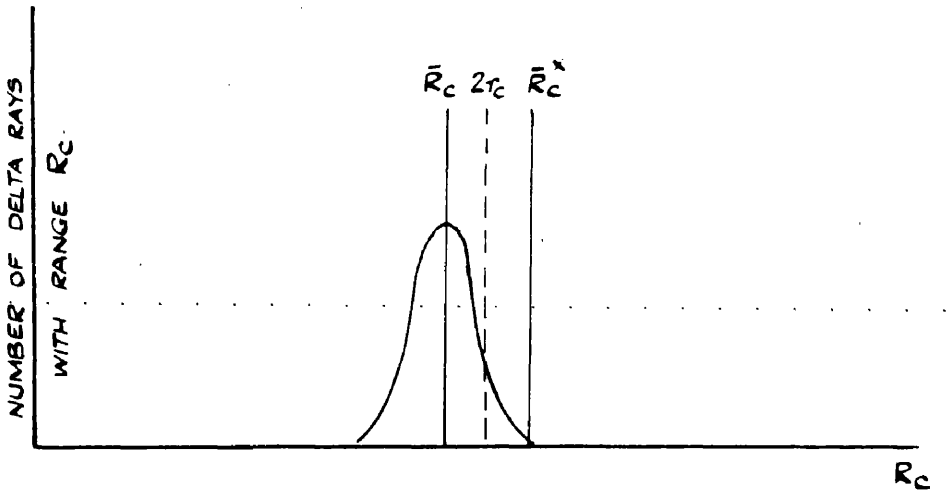

Figure 20 (a). Case III(a). $\bar{R}_c < 2r_c < \bar{R}_c^x$.

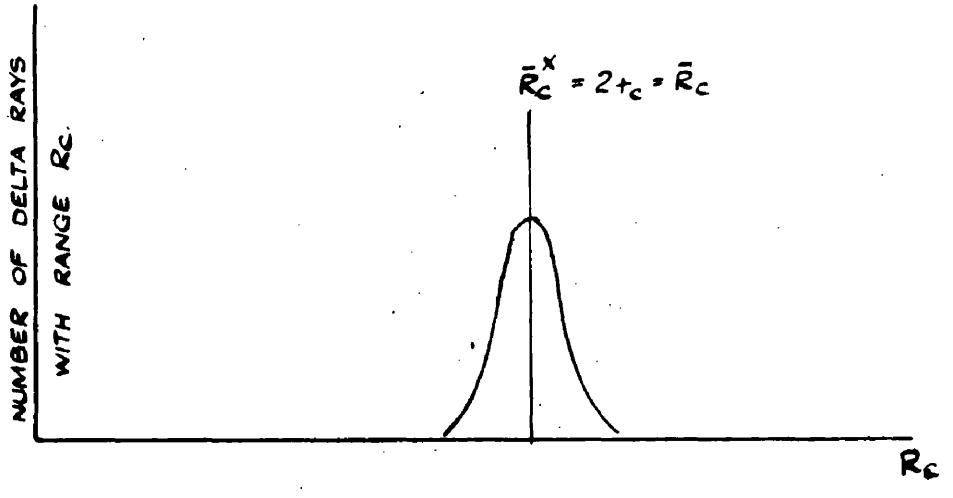

Figure 20 (b). Case III(b). $\bar{R}_c = 2r_c = \bar{R}_c^x$

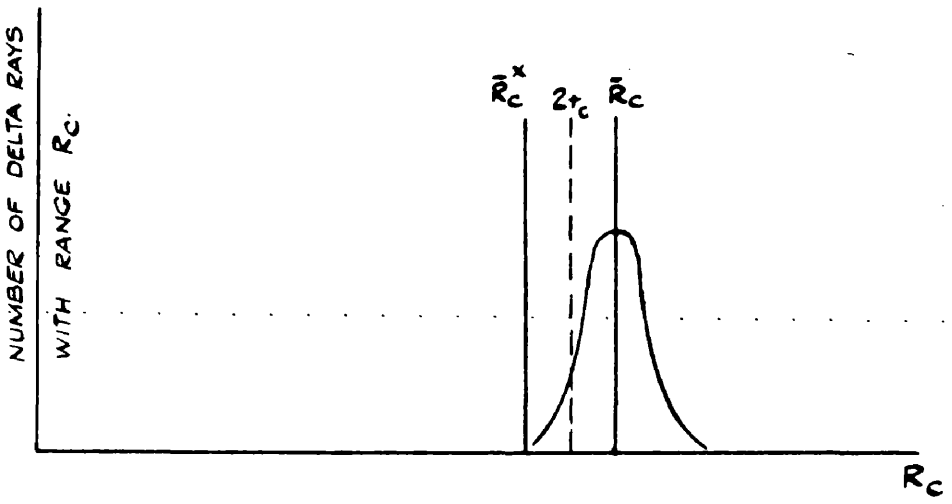

Figure 20 (c). Case III(c). $\bar{R}_c > 2r_c > \bar{R}_c^x$.

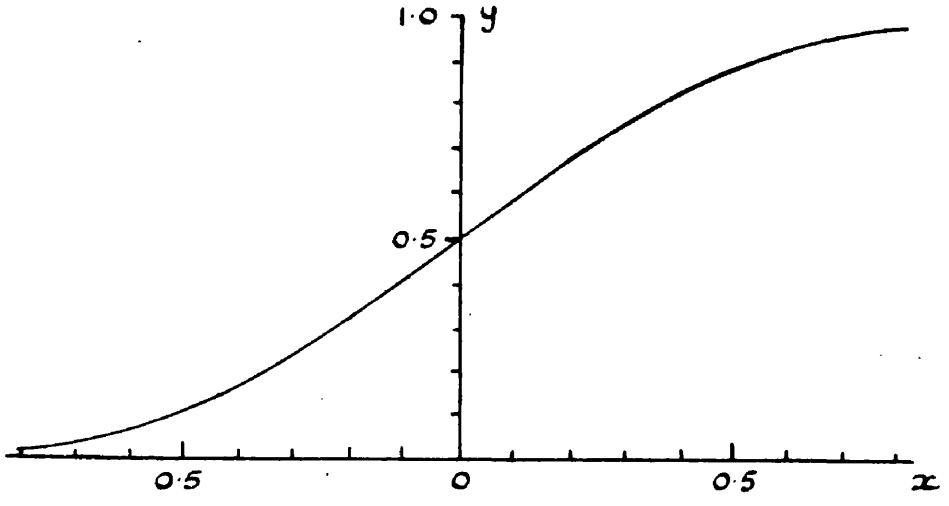

Figure 21.
The function $y = \frac{1}{\sqrt{\pi}} \int_{-\infty}^{x} e^{-\frac{1}{2}t^2} dt$ (see equation (17)).

where $x = (2r_c - \bar{R}_c)/a$ and $a = (\sqrt{2}/.6745) \times$ the half width of the gaussian distribution.

When $\bar{R}_c < 2r_c < \bar{R}_c^x$, fig. 20 (a), x is positive;

when $\bar{R}_c = 2r_c = \bar{R}_c^x$, fig. 20 (b), x is zero; and when

$\bar{R}_c > 2r_c > \bar{R}_c^x$, fig. 20 (c), x is negative.

IV. In general.

The number of bubbles/cm. = (17)

$$n_s(\alpha E_c) \propto \frac{1}{\sqrt{\pi}} \int_{-\infty}^{x} e^{-\frac{1}{2}t^2} dt$$

where $x = (2r_c - \bar{R}_c)/a$, a is defined above and $n_s(\alpha E_c)$ is given by equation (14).

For $2r_c \ll \bar{R}_c^x$, i.e. for high temperatures, $2r_c$ is much greater than the corresponding $\bar{R}_c$, x is large and positive, and the integral is nearly unity, hence the number of bubbles follows the curve given by equation (14). For $2r_c \gg \bar{R}_c^x$, i.e. for low temperatures, $2r_c$ is much smaller than the corresponding $\bar{R}_c$, x is large and negative, and the integral is nearly zero, hence no bubbles are formed at low temperatures.

Between these extremes the function $y = \frac{1}{\sqrt{\pi}} \int_{-\infty}^{x} e^{-t^2} dt$ (see figure 21) is superimposed on the curve of equation (14).

Comparison with experiment.

By normalisation to the measurement of bubble density with varying temperature in isopentane, the half width of the distribution and the threshold value $\bar{R}_c^X$ can be calculated. Fig. 22 shows the theory (equation (17)) and the experimental points; this is given by a half width of $4.2 \pm .2$ Å and a threshold range of $167.8 \pm .2$ Å, that is a spread of $2.5 \pm .1$ per cent in the range.

The theory can be further tested by applying equation (17), with the same values of α and a, to the result of measurements of bubble density with varying bottom pressure and fig. 23 shows equation (17) plotted on this graph.

The only other similar results are those of Blinov, of Glaser, of Bassi and of Chapter III. Unfortunately Blinov did not publish an accurate value of the temperature of operation of the chamber in which his measurements were made, and, as is usual with earlier 'dirty' chambers, the pressures in the other cases were not known. However a good fit is obtained for these results by assuming likely values for temperature and pressure.

Looking now at the foundations of the above theory, it has been assumed that there is a

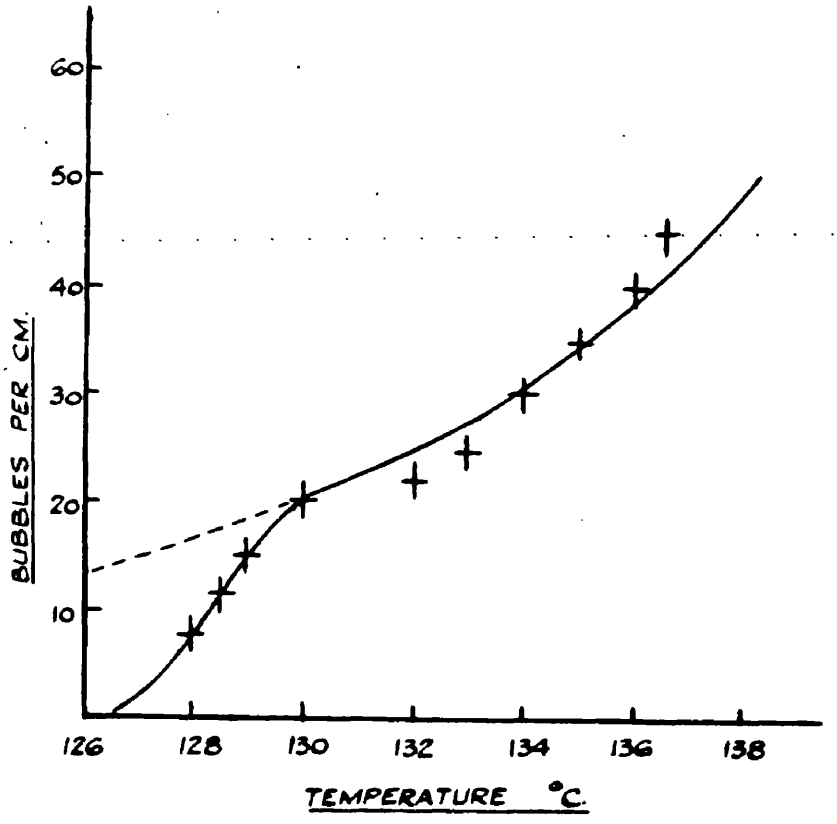

Figure 22. Equation (17) compared with the experimental results of fig. 6. The dotted line is equation (14) of fig. 17.

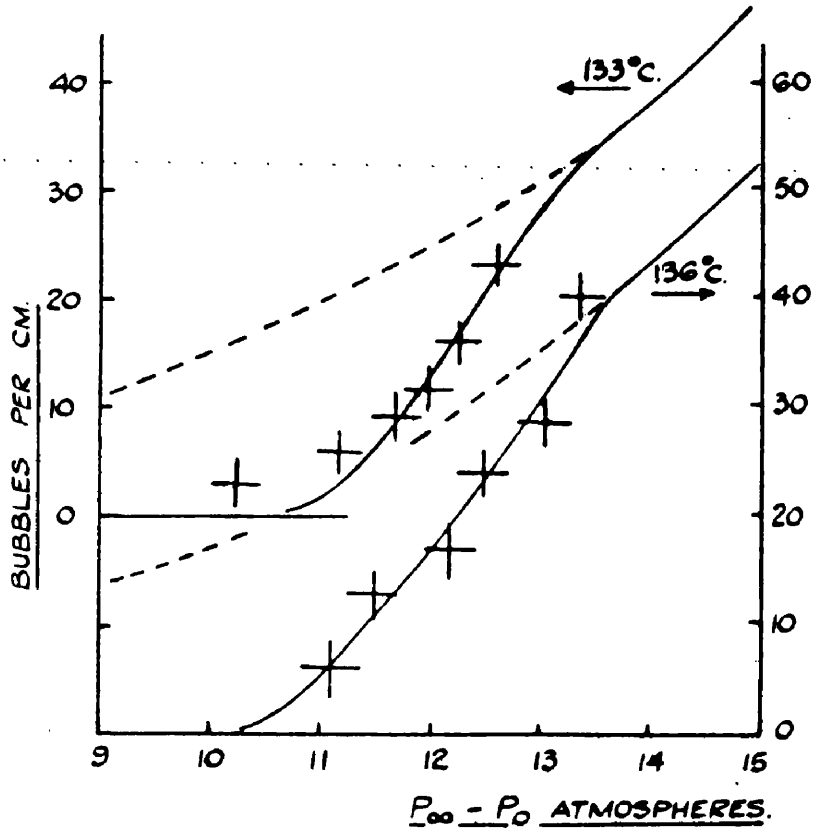

Figure 23. Equation (17) compared with the experimental results of fig. 7. The dotted lines represent equation (14).

'threshold' of the chamber sensitivity for a bubble chamber. This threshold is not an absolute barrier but there is a probability distribution (gaussian) operating in the region. It has seemed reasonable to attribute the uncertainty to variations in the range of the delta ray forming the bubble. This is perhaps the weakest point in the theory as there are many other reasons that may cause uncertainty in the initial stages of formation. However it is only necessary to accept some uncertainty for the rest of the theory to follow.

The justification of the above assumptions is that, after normalisation to one result, the theory is a good fit to the other available experimental evidence.

Normalising the results to the experimental evidence required the assumption of the following δ-ray ranges corresponding to the stated energies.

Range (Å).	Energy (eV).
167.8	2595
163.6	2450
147.0	1950
140.0	1720

These results lie on a smooth curve, approximately

$R \propto \sqrt{E}$, but cover too small a region for an equation of the form $R = f(N,Z,E)$ to be postulated with any confidence. The range of low energy electrons in this foils of aluminium has been measured by Glendenin (ref.14) and found to follow the law $R \propto E^2$ within experimental error between the energies 10 KeV and 100 KeV. It would appear reasonable to extrapolate this law to lower energies where direct measurements cannot be made.

The range predicted for, say, a 2600 eV electron with least straggling is 650 Å (compared with about 180 Å found above); this is only of the order of a few times the intermolecular distance in the medium. The extrapolation cannot be expected to be valid when the assumed uniform distribution of identically bound electrons becomes untenable.

At such low energies and in such complex molecules as pentane and propane the electrons might be expected to interact with many orbital electrons in one molecule and a precise treatment of the subsequent energy losses would be difficult. Intuitively this effect would tend to shorten the 'range' of such electrons.

Conclusions.

In the light of the above theory the unexplained characteristics of the bubble density results easily fall into place. The 'plateau' is caused by a fall off in sensitivity as the critical diameter approaches the mean range of the delta-rays with sufficient energy to form the bubble. This causes a point of inflexion in the curve in the region where E_c, and hence $\propto E_c$, (from equation (11)), is a slowly varying function of temperature leading to an apparent plateau.

The dependence of the temperature at which bubbles first appear, as a function of pressure, is now explained by the fact that for given particles and liquids the controlling factor is

$$\overline{R}_c^x = 2\, r_c = 2 \times \frac{2\sigma}{P_\infty - P_o}$$

Thus to estimate the working temperature and pressure of a given liquid it is necessary to calculate the value of E_c for different conditions and to solve equation (15). Since E_c varies very little for hydrocarbons this condition is approximately equivalent to $\overline{R}_c^x = 180$ Å, that is $r_c = 90$ Å. This is valid for isopentane and propane.

When more results are available from liquids such as methyl iodide, tungsten hexafluoride,

helium and hydrogen a check can be made on the above theory. The necessary physical constants for liquid hydrogen and helium are not sufficiently well known for results to be applied at present.

Chapter VI. APPLICATION OF THE BUBBLE CHAMBER.

Selection of problems.

Having achieved the object of photographing bubble chamber tracks and having made a very full investigation of the factors which control the nature of these tracks it remains to apply the technique to suitable problems.

In the introduction the bubble chamber was compared with other particle detectors and it is apparent that the most important advantage it has over the others is that it provides a high density target material in which the origin of events may be observed. This means that the primary field of usefulness of the technique is in the investigation of nuclear reactions caused by the bombardment of the chamber liquid by high energy photons, mesons or nucleons.

Most of the other uses of the bubble chamber, for example detection of particles from a target in a particle or photon beam, can also be done by one or more of the other detectors available; mainly, for the same range of energies, by nuclear emulsions

or crystal scintillators.

The range of energies for which a bubble chamber is suitable depends on the size of the chamber and on the nature of the filling liquid. In general such processes as proton-proton scattering, meson scattering, meson production and meson decay are within the scope of the technique.

Photoproduction of mesons.

Since 1935 the most important avenue of research into the structure of matter has been the investigation of the structure of the nucleus. By many scattering experiments the 'size' of the nucleas, or rather the range of the purely nuclear forces, has been closely defined. The exchange nature, the saturation properties and the non-central effects of the nuclear force have yet to be fully understood.

It is now well established that the π-meson, and perhaps other mesons, are intimately connected with the forces between nucleons. π-mesons may be emitted, scattered or absorbed by nuclei, and it is by the further investigation of these processes that knowledge can be gained of the structure of the nucleus.

Since mesons may be created in a nuclear reaction where there is sufficient energy available,

their production can be studied by the bombardment of nuclei by high energy protons or photons. The most important targets for this purpose are the simplest ones, protons, deuterons and helium nuclei.

The deuteron is a target of especial interest as it represents the simplest interaction of two nucleons.

Mesons are the 'quanta' of the nuclear force field, the observation of their creation in a nucleus might, therefore, be expected to lead to important results in analogy to the observation of spectra from excited atomic structures. To excite the nucleus, in a controlled manner, a nucleus can be given energy by a collision with an artificially accelerated particle or by absorbing an artifically produced high energy photon.

This leads to the particular application of a hydrocarbon filled bubble chamber to the detection of photoproduced mesons.

The chamber as a target.

The quantities which it is important to measure are, the cross-section of the $h\nu$ + nucleon $\rightarrow \pi^{\pm}$ + nucleon process, and the energy and angular distribution of the mesons. To accomplish this the bubble chamber

may be used in two ways, in the first case simply as a detector observing mesons produced in an external target in the photon beam or secondly as both detector and target. The scope of the second application is wider for the following reasons.

The cross-section for the photoproduction of mesons in hydrogen, carbon and similar 'light' targets is low and therefore only in a thick target will a sufficient number of events occur. The thickness of a target is usually a compromise between its total reaction cross-section and its stopping power for particles produced in it. That is, any particle emerging from the target has an uncertainty in its determined energy at origin equivalent to the thickness of the target. This disadvantage of a thick target is not present in the bubble chamber, in which the target and the detecting medium are identical.

Also the measurement of the angular distribution is considerably simplified by passing the incident beam through the detector. The chamber provides detection of the particles produced in a total solid angle close to 4π steradians enabling the complete distribution to be obtained

without altering the position of the detector. This has the added advantage, over alternative methods, that the conditions of the experiment cannot alter when observation is made at different angles.

The problem of electron background.

Since the collimated γ-ray beam of the synchrotron will produce a dense core of electrons in the chamber, the success of any experiment involving meson or proton detection in the chamber will depend on the ease of distinction of these particles against the background of electrons. It is important therefore to determine the conditions of operation which give maximum contrast between the electrons and the heavier particles. The suppression of electrons by lowering the sensitivity of the chamber will not in all cases be desirable as it is often necessary to observe the decay electron from a μ-meson in order positively to identify a meson. However as this is such a characteristic decay process only a faintly discernible electron track is necessary. Another important factor which will be dependent on the sensitivity of the chamber and on the size of the

photographed bubble is the degree to which the core is 'transparent'. The density of the core will determine the lower energy limit of particles which may be observed when produced in the beam and will also affect the range of angles at which short tracks may be observed.

The two main parameters over which the operator has control are bubble density and bubble size. Varying either of these can alter the contrast between, for instance, meson and electron tracks. Close to maximum contrast is obtained when the bubble diameter, of bubbles formed by the meson, is equal to the distance between bubble centres; that is the meson track is almost a continuous row of bubbles whereas the electron track is apparently thinner. A change of conditions which increases the bubble density will bring electron tracks closer in appearance to meson tracks, which will be relatively unaffected. In establishing the optimum chamber conditions due allowance must be made for variations in heavy particle energy along the track and in general the conditions should suit the particular requirements of the observation.

For studying photon induced events in a hydrocarbon bubble chamber the problem becomes one of the relative magnitude of the cross-sections for pair production and the cross-section for useful measurable events. There is no upper limit on the size of bubble chamber which would be useful so it was decided to build a 10" diameter 4" deep cylindrical bubble chamber which would provide information on photoproduced mesons between 5 and 35 MeV. The chamber would be propane filled and would require thin windows for entry and exit of the γ-ray beam.

The γ-ray beam of the 340 MeV synchrotron has a maximum intensity of the order of 5×10^6 equivalent quanta per pulse. If the full beam, approximately 3 cm in diameter, were allowed to pass through the propane filled chamber it would produce in the chamber 500 π-mesons between the range of 1 cm and 10 cm and about 1.5×10^6 electron pairs between the energies of 10 and 300 MeV. Since even a 10 MeV electron has a range of 6 cm in propane, all of these electrons would contribute to the background against which events must be visible. These electrons are produced in a predominantly forward direction

and form a pencil of tracks along the path of the beam whereas mesons would have an approximately isotropic distribution. Obviously such a flux of electrons would tax the sensitivity of the chamber. Some reduction in the beam is therefore necessary and if simultaneously the electrons can be confined to a narrow pencil it might still be possible to trace to the point of origin particles produced in the beam.

The effect which a photon beam produces in a liquid hydrogen bubble chamber has been observed by Gates (ref.15) but no similar experiments with other liquids have been reported. This means that the potentialities of the hydrocarbon medium and the disadvantages it suffers from increased pair production are largely unknown.

Chapter VII. A 5-LITRE CHAMBER FOR THE STUDY OF PHOTOMESON PRODUCTION.

Chamber Design.

The problems associated with designing a large hydrocarbon bubble chamber centre mainly on the strength of the parts and the sealing of the vessel against high pressure.

For example the glass windows are subjected to a pressure of 500 p.s.i. over an area of 10" diameter and thus have a total force on them of about 18 tons weight which is repeatedly released and applied. The glass, the ring securing it, and the retaining bolts have to stand this stress with a margin of safety. The manufacturers of 'Armour-plate' recommended and supplied windows $1\frac{1}{2}$" thick 12" diameter to be secured by a ring overlapping the glass by 1".

It was decided to manufacture the body of the chamber of brass, and it is essentially a cylinder, outside diameter $13\frac{1}{2}$ in., internal diameter 10 in., depth 4 in. (fig.24). Two diametrically opposite holes of 1 in. diameter are cut in the casting to provide windows for beam entry and exit. It was originally intended to construct these windows of terylene sheet about .015 in. thick

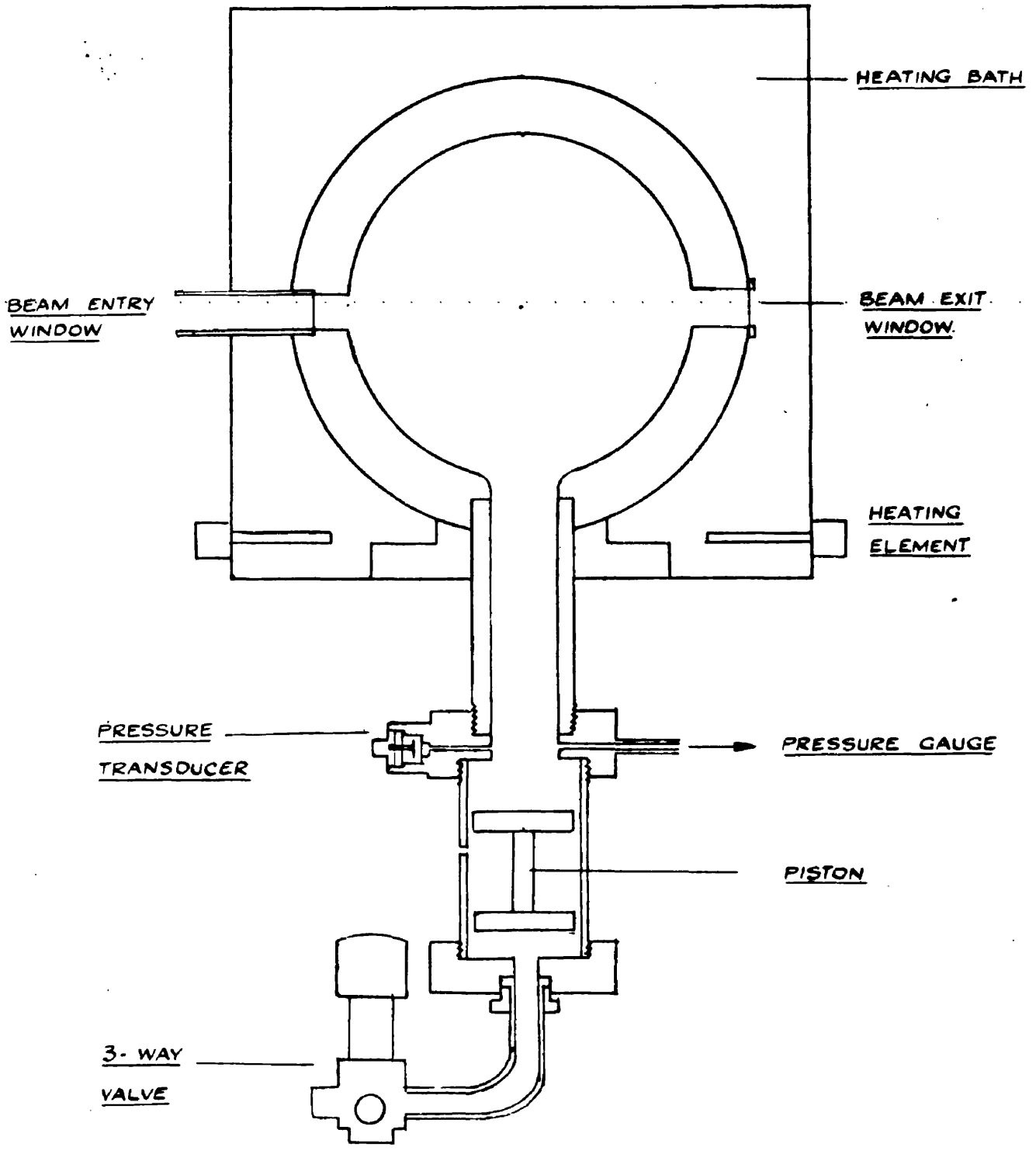

Figure 24. Diagram of the 5-litre 'dirty' chamber, showing thin beam entry and exit windows.

covering a hole $\frac{1}{4}$" in diameter. However the advantage gained in using this material of low atomic number is not sufficient to warrant the risk of failure of the thin window. Therefore these windows were made from .015 in. thick copper-beryllium foil which supports the required pressure over a window 1" in diameter.

Expansion of the chamber is effected through a 2 in. diameter pipe which is hard soldered into the brass casting. The pipe extends 8 in. from the chamber and is threaded for connection to the expansion apparatus. The junction between the casting and the pipe has to suffer considerable strain during expansion since it is also used to support the weight of the chamber. This pipe passes vertically through the floor of the heating box, through a watertight O - ring seal.

The capacity of the chamber thus designed is 5 litres of propane. An expansion of about 5% volume change is necessary to obtain the correct superheat — that is a change of volume of 250 cc. The method chosen to achieve this expansion consists of a $3\frac{1}{2}$ in. diameter piston moving in a cylinder with a stroke of 2 in. The cylinder is attached to the chamber by a connecting piece which contains a

pressure transducer, provision for the attachment of the filling apparatus and a static pressure guage.

The expansion valve which allows rapid exhaust of the cylinder is a 3-way solenoid operated valve with $\frac{3}{4}$ in. diameter ports. Nitrogen gas is supplied at about 400 pounds per square inch to the inlet port of this valve and the normal unenergised position of the valve allows this pressure to compress the chamber. The alternative position of the valve exhausts the cylinder to atmosphere.

The chamber is heated in a water bath (fig.25) with 'triplex' glass windows. Special provision is made to allow the γ-ray beam to pass directly into the thin window of the bubble chamber. Two 1.5 kilowatt electric elements maintain the temperature at a level determined by the applied voltage which is controlled by a 'Variac' transformer. The bath is provided with a gas tight lid so that any escaped propane can be led safely away. Temperatures are measured in the bath by mercury-in-glass thermometers.

For the purpose of stereo-photography two 35 m.m. cameras are mounted 10" apart 20" from the front glass of the chamber (fig.26). The cameras are inclined slightly so that the centre of the chamber coincides with the centre of the photograph.

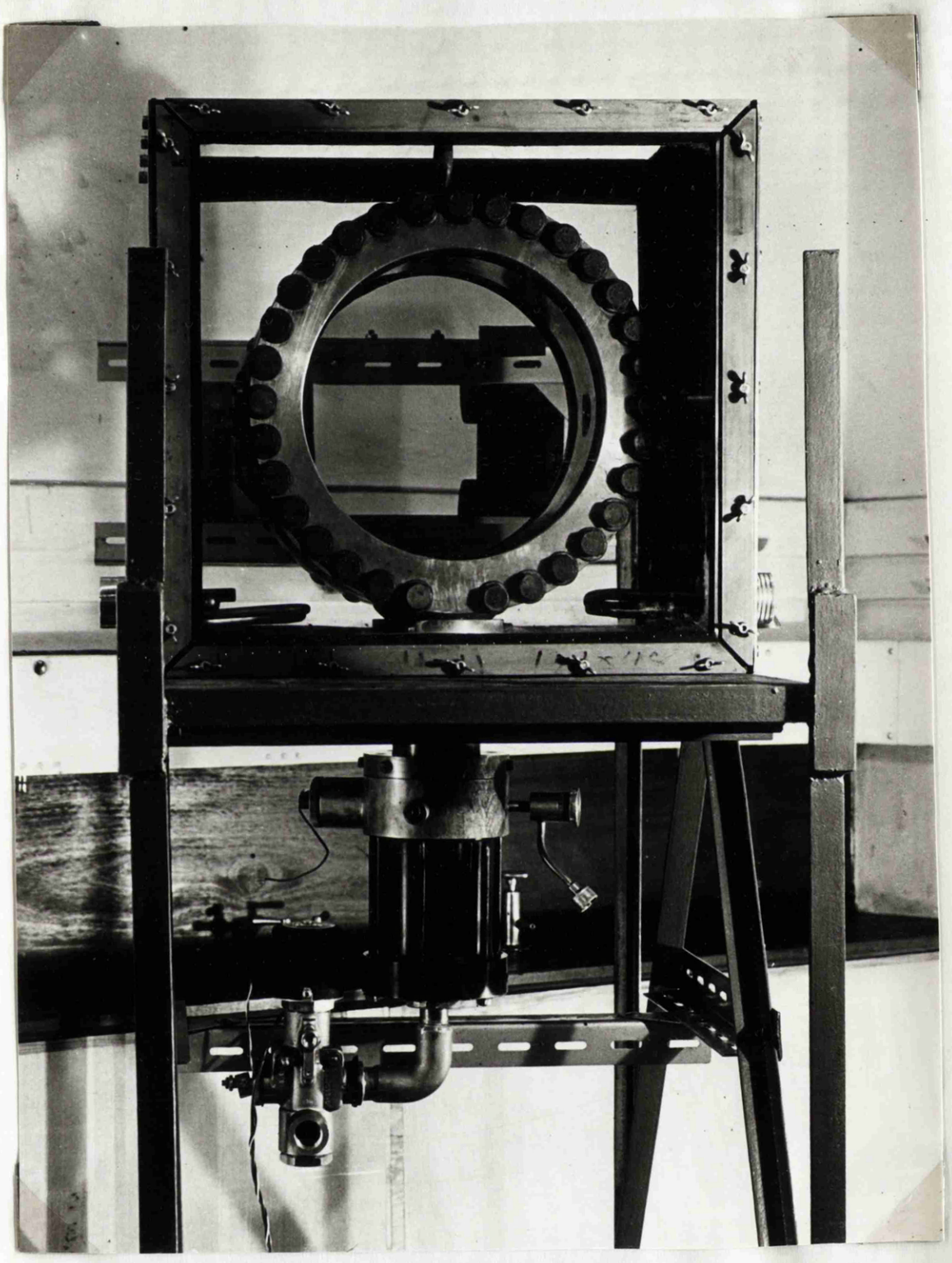

Figure 25. The 5-litre chamber.

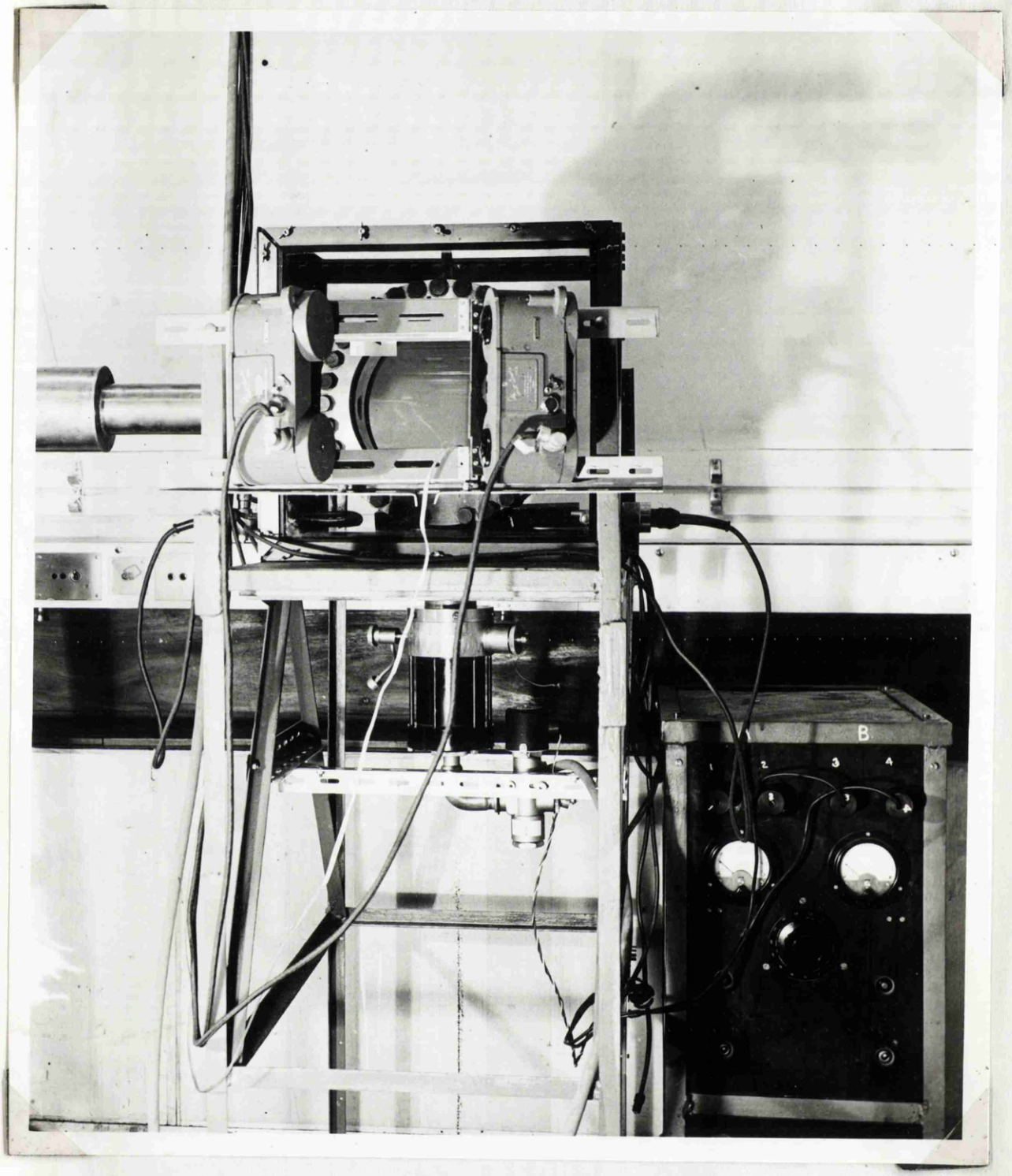

Figure 26. The 5-litre chamber showing the position of the two 35mm. cameras.

At a lens stop of f11 adequate depth of focus is obtained. It is possible to use both dark field and bright field illumination. Bright field illumination is obtained by having a diffusing screen behind the chamber which is illuminated, through condensing lenses, by the lamps . This method gives poor contrast but permits measurements of bubble diameter and accurate positioning of bubble centres. In dark field illumination light is allowed to fall on the bubbles in the chamber without striking the camera lenses. Since light scattered by bubbles is mainly in the forward direction the angle between the incident light and the line between bubble and camera is made as small as possible.

The latter method is preferred because of the higher contrast obtainable. Two flash lamps are placed behind the chamber and the camera views a black velvet screen behind the chamber.

The chamber, thus designed, was ready for preliminary experiments necessary to determine the characteristics and operating conditions suitable for this particular chamber, leading to information of importance to other experimenters in this field.

Testing the chamber.

The conditions of operation may vary between chambers depending on the amount of wall boiling present and the speed of the expansion. Amongst the characteristics of the chamber, which require to be investigated, is the duration of sensitivity; this is the time during which ionising particles entering the chamber will produce tracks and occurs at the time of maximum superheat and lasts for 3 to 15 milliseconds depending again on the wall boiling and the speed and amount of the expansion. Also the time taken to cycle the chamber is an important characteristic which will depend on the conductivity of the chamber wall and on the amount of vapour to be recondensed.

A convenient method of testing a chamber under conditions of operation is to observe Compton electrons produced in the chamber by γ-rays from a radioactive source such as Co^{60} which emits 1.3 MeV and 1.1 MeV γ-rays. Such a source, of about 10^6 γ-rays per second, was placed close to the beam entry window of the chamber. The chamber was operated and photographs were taken with the illumination triggered at various times during

and after the sensitive time of the chamber. As would be expected later flash times revealed greater number of bubbles although there was little variation in bubble size i.e. bubble growth was slow. Fig. 27 shows a photograph of bubbles produced by the Compton electrons, taken 5 milliseconds from the beginning of the sensitive time. The sensitive time was found to last about 25 milliseconds.

Since it is useful to know the lowest pressure achieved during the expansion, the pressure transducer used on this chamber was of a design which made possible its measurement. The bottom pressure was observed to be 9.6 atmospheres when the saturated vapour pressure was 18.2 atmospheres and therefore a superheat of 8.6 atmospheres was obtained. (Subsequent polishing of the chamber and modifications of the piston made possible superheats of up to 11 atmospheres).

Operation with the synchrotron.

For operation of the chamber with the 340 MeV synchrotron a pulse, 80 milliseconds before the beam, is delayed about 40 milliseconds before triggering the chamber expansion which has an inherent mechanical delay of about 40 milliseconds. The

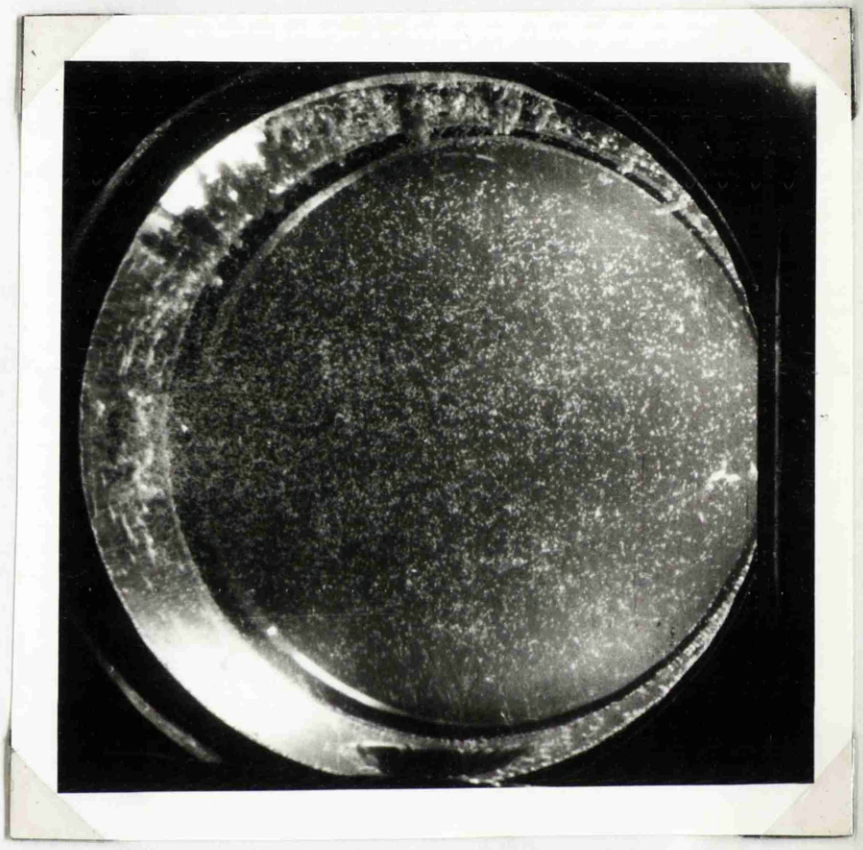

Figure 27. Bubbles produced by Compton electrons initiated in the 5-litre chamber by Y-rays from a cobalt-60 source. Such photographs were taken to determine the operating conditions of the chamber.

same pulse is delayed about 81 milliseconds to trigger the lamp flash for the photograph. This requires two very stable delay circuits, preferably stable to within 1 ms in 80 ms for which a modified phantastron circuit is used. The current for the magnetically operated expansion valve is controlled by an output pentode and a square pulse generator. The lamps used are two argon filled LSD 16 tubes and the discharge of 50μF at 1.5 KV which operates them is triggered by a suitable pulse from the delay circuit.

The sequence of events is monitored on two oscilloscopes enabling accurate control and measurement of the times involved.

Collimation of the γ-ray beam.

To limit the core of electrons produced in the chamber by the synchrotron beam it was decided to reduce the diameter of the beam to about 1/8 in. so that most of the electron pairs would be confined to a narrow pencil in the centre of the chamber. This was the smallest the beam could be conveniently made without reducing the cross-section for meson production to an unworkable value. With this

geometry an average of 2 mesons between the energies of 5 MeV and 35 MeV should be observed per picture. A greater cross-section would of course be desirable but the 1/8 in. beam was thought to be suitable for a preliminary experiment.

The γ-ray beam of the synchrotron is collinated close to the target of the machine by a lead collimator with a $\frac{1}{4}$in. diameter hole, the beam then spreads out in a cone reaching a diameter of about 1" at the position of the bubble chamber collimator. This latter collimator, a lead cylinder length 9", effectively absorbs the beam allowing only a narrow $\frac{1}{8}$" diameter γ-ray beam to pass into the chamber (fig. 28). To reduce the number of electrons which enter the chamber a magnetic field of about 10,000 gauss is applied over a distance of 3 ft. between the $\frac{1}{8}$" collimator and the chamber. In this way electrons already present in the beam and electrons produced in the collimator are deflected out of the beam and are absorbed by lead surrounding the chamber entry window. It was unnecessary to provide an air free path for the beam between the synchrotron target and the chamber since the first cm. or so of propane has an equivalent cross-section for pair production.

An ionisation chamber behind the bubble chamber monitors the beam intensity.

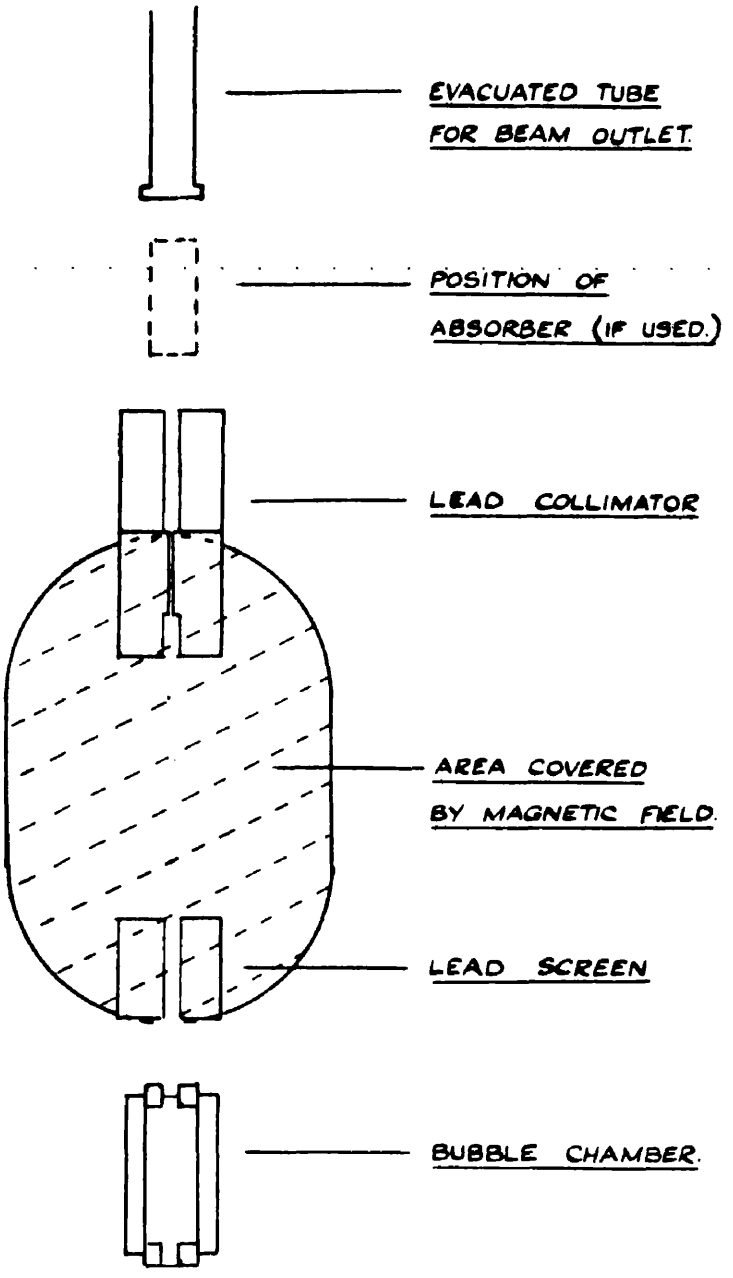

Figure 28. Diagram illustrating the method used to collimate the synchrotron beam.

Chapter VIII. A STUDY OF METHODS FOR THE REDUCTION OF BACKGROUND.

Measurement of range.

For an experiment which investigates the properties of photoproduced π-mesons, from carbon or hydrogen nuclei, the requirements are accurately measured meson energies and accurately defined directions of the produced mesons so that the dynamics of the reaction may be reconstructed. The measurement of energy is the more exacting of these with regard to track quality and thus this measurement sets the criterion for conditions of operation. The simplest method of measuring the energy is to make a measurement of the range which can be related to the energy through results of other experimenters. The range is accurately defined if each end of the meson track is visible in the chamber by two cameras. It may not always be possible to distinguish the origin of the track in the case of electron pairs and there is some inaccuracy in assuming the reaction to have taken place on the centre line of a γ-ray beam.

For a precise measurement of the range the core must be 'transparent'. That is, the electron must produce tracks of low bubble density so that other tracks, possibly of mesons of energy as high as

40 MeV, may be observed at their origin in the γ-ray beam. This proves to be difficult as the meson is almost without exception lightly ionising at its origin and the electron tracks are numerous. Just how much of an obstacle this situation presents is the main reason for the investigations carried out with the propane bubble chamber.

It is obvious that the ideal conditions are met with the meson track just discernable at its origin; that is, the conditions of operation must be such that ionising particles produce a relatively low bubble density and the bubbles must be photographed when they are quite small. These two conditions may be varied independently. When the best conditions have been determined there will be a maximum tolerable beam intensity. The number of photographs which have to be taken to collect the required information will depend on this value of tolerable beam intensity.

Photographs were taken with the arrangement described above. Variations were made in the sensitivity of the chamber, affecting bubble density, in the lamp delay, affecting bubble size, and in the incident beam intensity.

Variation of chamber sensitivity.

Since the bottom pressure P_o is not easily variable, being determined by the nature of the expansion mechanism, it remained at a constant value of 9.6 atmospheres for the experiment. Bubble density, or sensitivity, was therefore varied by adjustments to the temperature of the bath surrounding the chamber.

The effect of temperature on the photograph can be seen by comparing figs. 29 (a) and (b) which were taken at temperatures 59.6°C and 61.0°C respectively. In fig. 29 (a) it can be seen that the electrons, which make up the 'core' of the beam, have not formed definite tracks whereas in fig.29 (b) they are observed as almost continuous lines. Fig. 29 (a) has a larger γ-ray flux, by a factor of about three, than (b) and so has more 'latent' electron tracks and yet does not appear any denser. This is a good example of the deliberate suppression of electron pairs while allowing the desired meson events to be clearly seen. (a) shows that a photoproduced π^--meson has interacted with a carbon nucleus producing a proton which stopped in the chamber. However, this beam is too intense for the origin of the meson to be distinguished.

Figure 29 (a). Tracks produced by the Y-ray beam at a chamber temperature of 59.6°C.

Figure 29 (b). Tracks produced by the γ-ray beam at a chamber temperature of 61.0°C.

Variation of lamp delay.

By reducing the time delay between the photon beam, which lasts only a few microseconds, and the lamp flash, it should be possible to reduce the observed bubble size to near the limit of photographic resolution. An improvement would then result in the 'transparency' of the core. The growth of bubbles, however, was found to be initially so rapid that the bubble size photographed in fig.30 (a) is the smallest which is practically possible before uncertainty in the time of flash (about ± 500 microseconds) causes photographs to be missed.

To illustrate the effect of a longer flash delay fig.30 (b) was taken with a delay of 8 milliseconds as compared with the 1 millisecond of (a). These photographs were taken under similar conditions of temperature and of γ-ray flux, showing that a later flash reveals bubbles to be much larger and the opaque region of the core more widespread. The boiling occasioned by roughness on the chamber walls can be seen to be in a more advanced state.

Variation of beam intensity

The only course remaining was to reduce the beam intensity until the origin of photoproduced

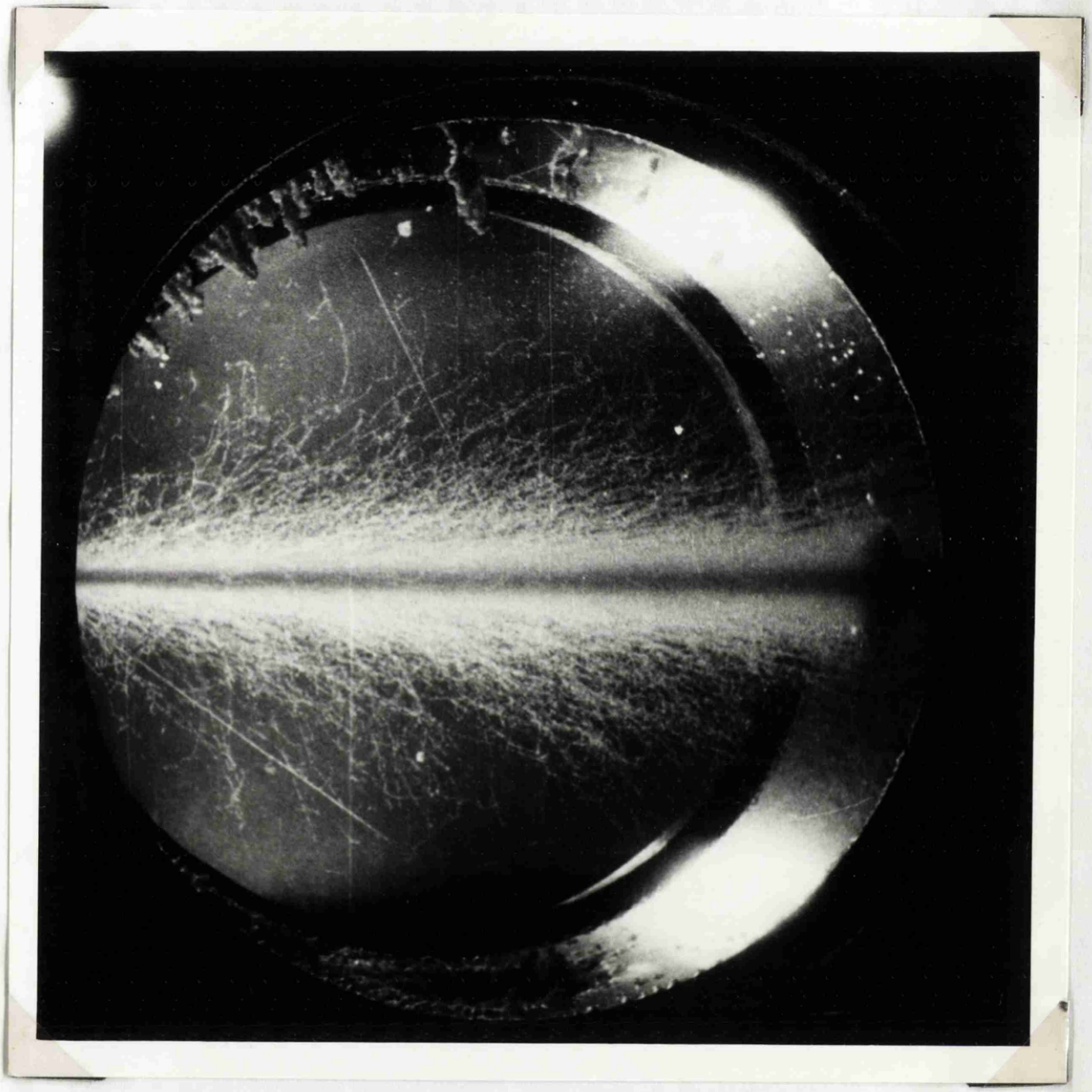

Figure 30 (a). Tracks photographed 1 millisecond after the passage of the beam.

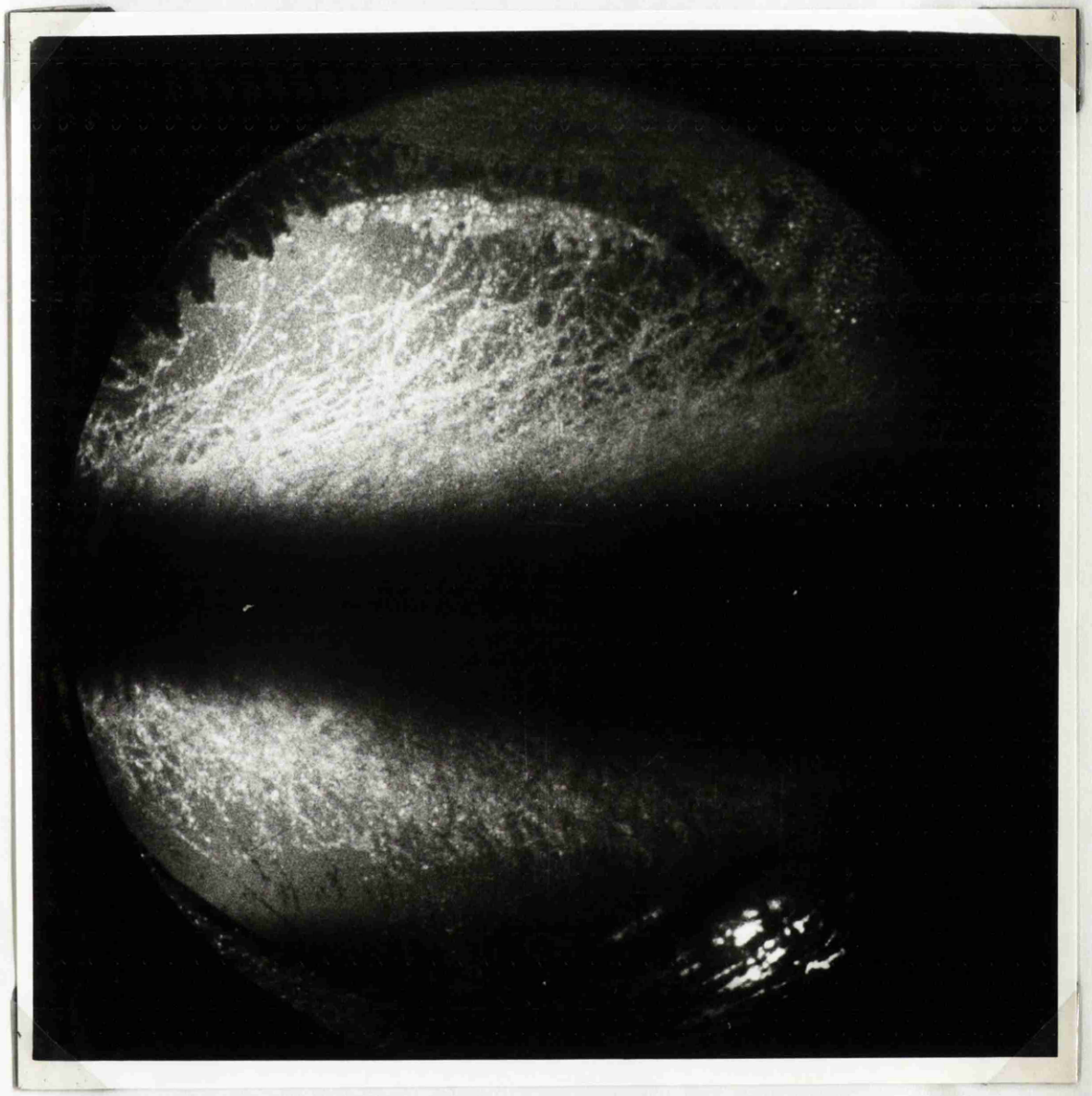

Figure 30 (b). Tracks photographed 8 milliseconds after the passage of the beam.

mesons could be seen in the core of electrons. The γ-ray beam was reduced by 'de-tuning' the synchrotron and many photographs similar to fig.31 were taken. It will be noticed in comparison with fig. 29 (a) that the beam has no shadow region, that is, there is no dark band representing a region not penetrated by the illumination. In spite of the reduction of a factor of four in beam intensity compared with fig. 29 (a) the origin of the meson (a similar reaction) is still indistinguishable.

The cross-section for the photoproduction of mesons in propane is such that the further reduction of the beam would make the experiment too demanding of synchrotron time. The rate of cycling of the chamber for these investigations averaged about one expansion every 40 seconds, but was often as rapid as every 10 seconds. Further reduction of the cycling time by faster recompression of the chamber will require modifications to the chamber. There is no reason why 5 cycles per second should not be achieved. The reduction of the γ-ray beam will therefore be possible to such low values that the small cross-section for the desired events will be compensated for by the number of photographs taken.

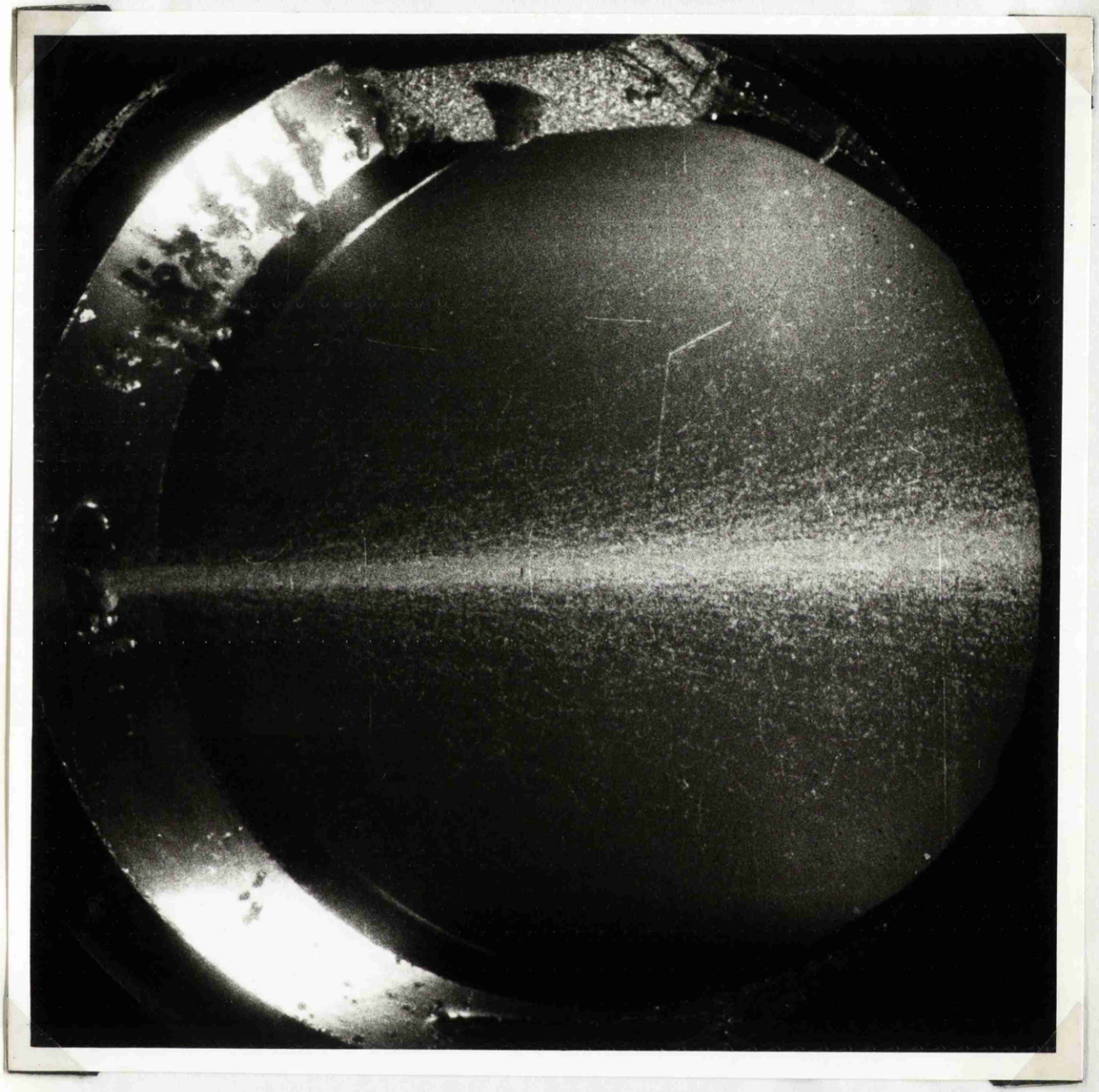

Figure 31. Photoproduction of a π^- -meson which reacts with a carbon atom ejecting a proton. The beam intensity is a factor of four lower than that of fig. 29(a). The 'core' of electrons has no shadow region but is not transparent.

Chapter IX. DISCUSSION.

Attenuation of the γ-ray beam.

It was first pointed out that attenuation of the synchrotron γ- beam was necessary if the chamber was not to be 'saturated' with tracks. The γ-ray flux was reduced, for the above investigation, by collimating the beam from an initial diameter of 1" to approximately $\frac{1}{8}$" diameter. This has resulted in the dense core of electrons being confined to a narrow pencil through the centre of the chamber. It appears, however, that it is still not possible to position the origin of an event with sufficient accuracy.

An alternative method of reducing the beam is simply to reduce the output of the synchrotron and allow the uncollimated beam to enter the chamber. By a reduction in intensity the core could be made sufficiently transparent to permit observations of the first bubbles in the track of a meson, or proton, produced by a reaction within the beam. The reduction of γ-ray flux would be offset by the larger area of the beam so that there would still be the required probability of events occurring in the chamber.

Since much of the troublesome electron background is produced by comparatively low energy electron pairs formed by photons of energy less than 150 MeV, which will not cause the photoproduction of mesons, it would be an advantage to reduce the low energy content of the γ-ray beam. This could be done by the use of absorbers of low atomic number e.g. CH_2 or LiH. The cross-section of these substances is considerably higher below 150 MeV than above. If the experiment involved the determination of the cross-section of elements in the bubble chamber, the use of these absorbers would complicate the calculations, but for the determination of π^+ to π^- production ratios or of angular distributions, etc., this problem would not be serious. Many electron pairs would be produced in the absorber itself and these would have to be removed from the beam by a strong magnetic field (fig. 28).

The necessity for such measures as this to improve the technique is only apparent as a result of the experiments described in the previous chapter.

Rapid Cycling.

If a chamber were recompressed within a few milliseconds of the photograph the complete cycle

of operation could take as little as 40 milliseconds Thus a compression and expansion system could be made to operate the chamber at 25 cycles per second. This is comparable with the pulse rate of most electron synchrotrons. Cycling rates of up to 1 per second have been obtained with the 5 litre chamber using a modified expansion apparatus.

A rapid cycling chamber synchronised with the pulsed beam of a synchrotron would be freed from restrictions on cross-sections and even with a small beam intensity would compete with counter techniques for most experiments.

So many photographs would be taken during an experiment that scanning might be tedious; however many research workers are developing and applying automatic scanning methods and analysis of the results by computers.

Targets within the chamber.

Most of the advantages of using the chamber liquid as the target material will apply to a target which is situated inside the chamber.

A gaseous target may be introduced into the chamber by constructing a pipe through the centre of the chamber along the axis of the beam. Such a pipe could be filled with any gas under considerable

pressure (ideally about 15 atmospheres) and could have quite thin walls. The target thus ppesented to the beam would have a low cross-section for pair production and the lowest energy electrons would be stopped in the pipe wall. The effect of the pipe wall on the energy of mesons entering the chamber from the beam could be calculated accurately and the uncertainty of the points of origin would be small in the gaseous medium. The most interesting targets, hydrogen, deuterium and helium, have low cross-sections for pair production, so this method would have an advantage over the use as a target of the hydrogen in the hydrocarbon, or of the deuterium in the deuteriated hydrocarbon.

A solid target may conveniently be placed inside the chamber in the form of a polished sphere or as a thin foil carefully mounted. Such a target would not materially increase the 'dirtiness' of the chamber compared with the already present wall boiling. The detection of particles from these targets would be very efficient giving acceptance over almost 4π steradians.

Conclusion.

The five years since the invention of the bubble chamber by Glaser in 1953 have seen a rapid advancement of the technique. It has already proved itself to be of great importance in observing the production and decay of heavy mesons. It is potentially valuable in the solution of many problems concerning nuclear structure and the "fundamental" particles. The bubble chamber may only be used to its fullest advantage when the basic processes involved in bubble formation are understood.

Much work has been done with liquid hydrogen chambers with strong magnetic fields so that the energy of particles may be calculated from their momentum. Considerably higher fields have to be used for hydrocarbon chambers in which particles suffer more scattering. The development of larger chambers and of chambers filled with liquids of high atomic number will make it increasingly difficult and expensive to obtain uniform fields of sufficient intensity in the chamber.

A knowledge of the equations governing the deposition of bubble forming nuclei along the

tracks of particles will enable velocity measurements to be made in the absence of magnetic fields. This method of energy determination would also be useful for short tracks in any chamber.

The experimental results, and their interpretation, in previous chapters, supply the basis of knowledge required for this technique. Further knowledge gained in these experiments has proved to be valuable in determining the optimum operating conditions when electron background is a problem.

The development of a chamber, and a collimating system through which a γ-ray beam of meson producing energy may be passed, has shown that this technique has a wide application and can be versatile in its use of solid, liquid or gaseous targets within the chamber.

References

1. Glaser D.A., Physical Review 87, 665 (1952).

2. Glaser D.A., Physical Review 91, 762 (1953).

3. Wood J.G., Physical Review 94, 731 (1954).

4. Hildebrand R.H., Proceedings 1954 Glasgow Conference on Nuclear and Meson Physics, 311.

5. Glaser D.A., et al., Physical Review 102, 1653 (1956).

6. Blinov G.A., et al., J.E.T.P. 3, 640 & 4, 661 (1956).

7. Glaser D.A., Rahm D.C., Il Nuovo Cimento 2, Sup.2, 361 (1954). Physical Review 97, 474 (1955).

8. Rahm D.C., et al., private communication.

9. Bertanza L., Martelli G., Tallini B., Il Nuovo Cimento 10,5, 940 (1957).

10. Glaser D.A., Handbuch der Physik XLV, 329.

11. Volmer M., Kinetik der Phasenbildung, Dresden 1939.

12. Seitz F., Physics of Fluids 1, 2 (1958).

13. Bassi P., et al., Il Nuovo Cimento, 5,4, 491 (1956).

14. Glendenin L.E., Nucleonics 2, 12 (1948).

15. Gates D.C., Swanson W.P., private communication.

ADDITIONAL PHOTOGRAPHS

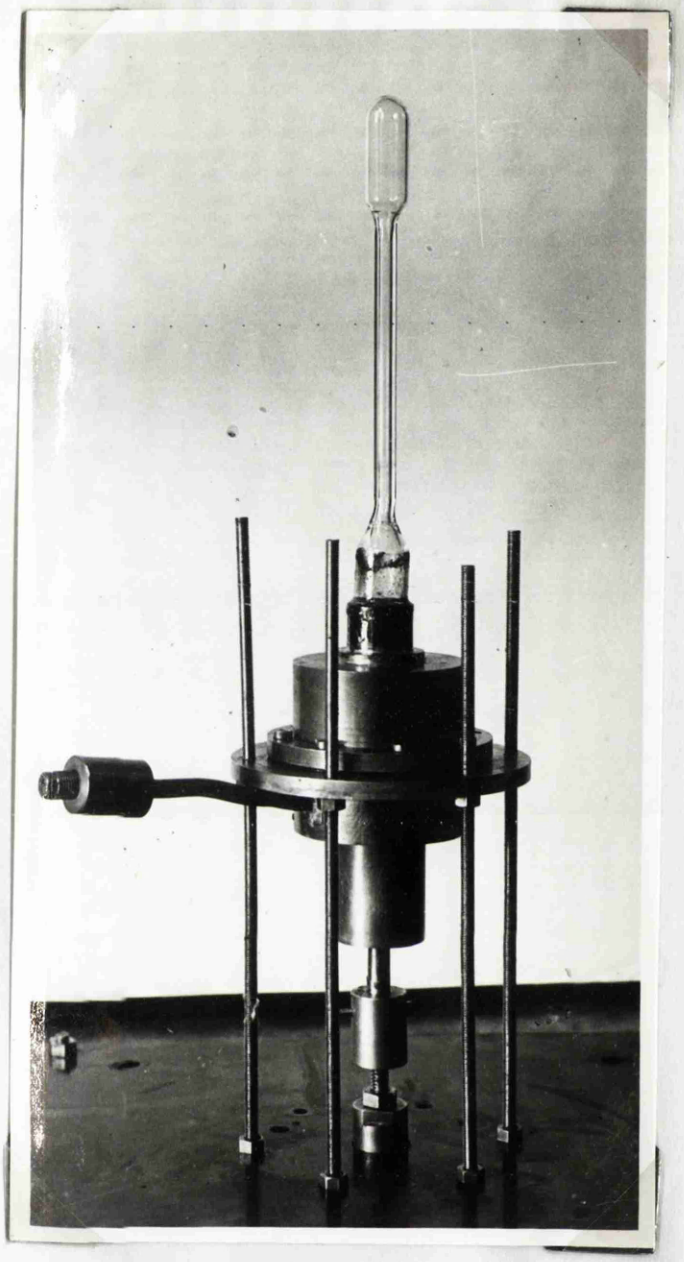

Plate (i). The 4cc. 'clean' chamber.

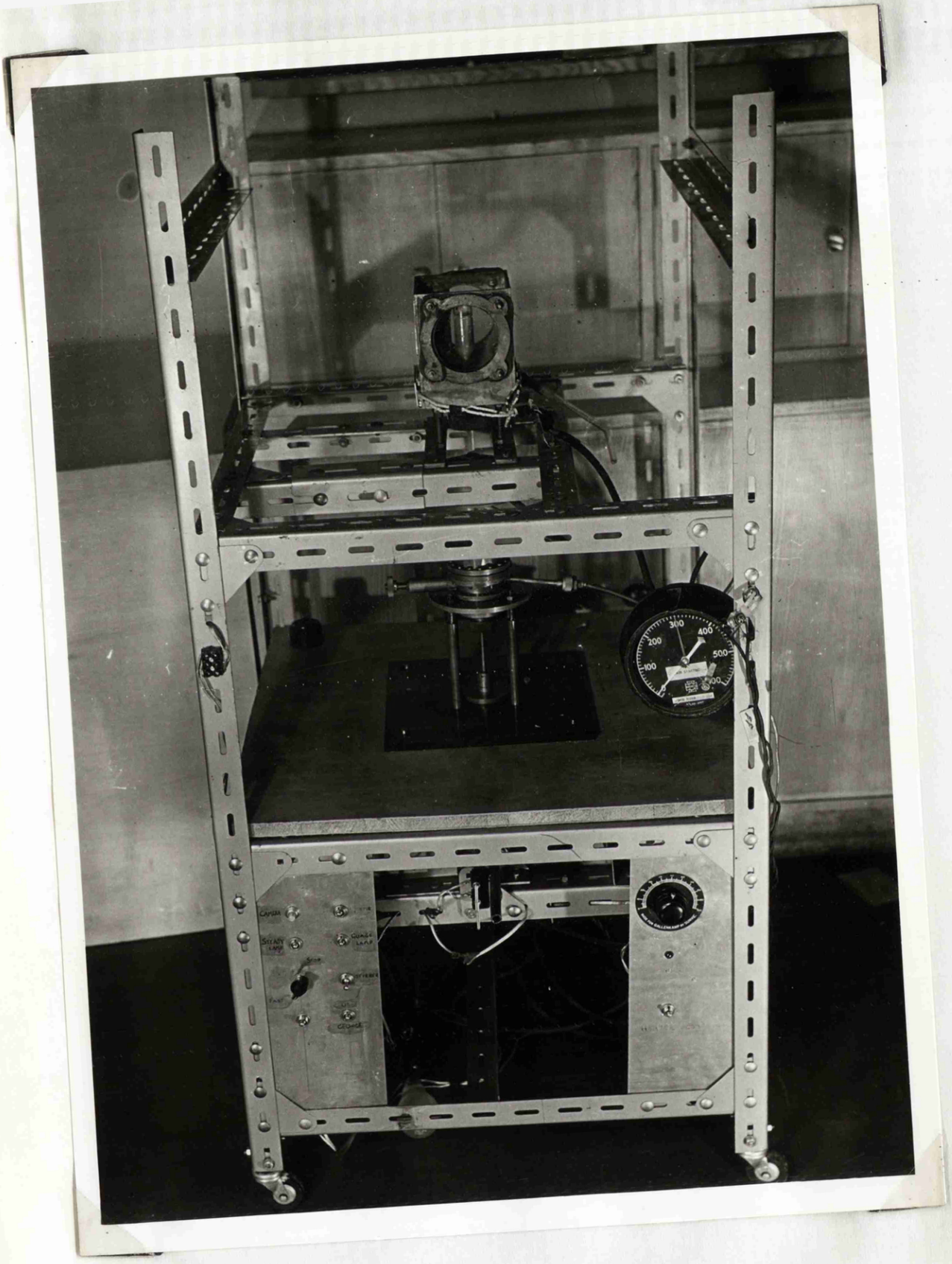

Plate (ii). The 20cc. 'clean' chamber.

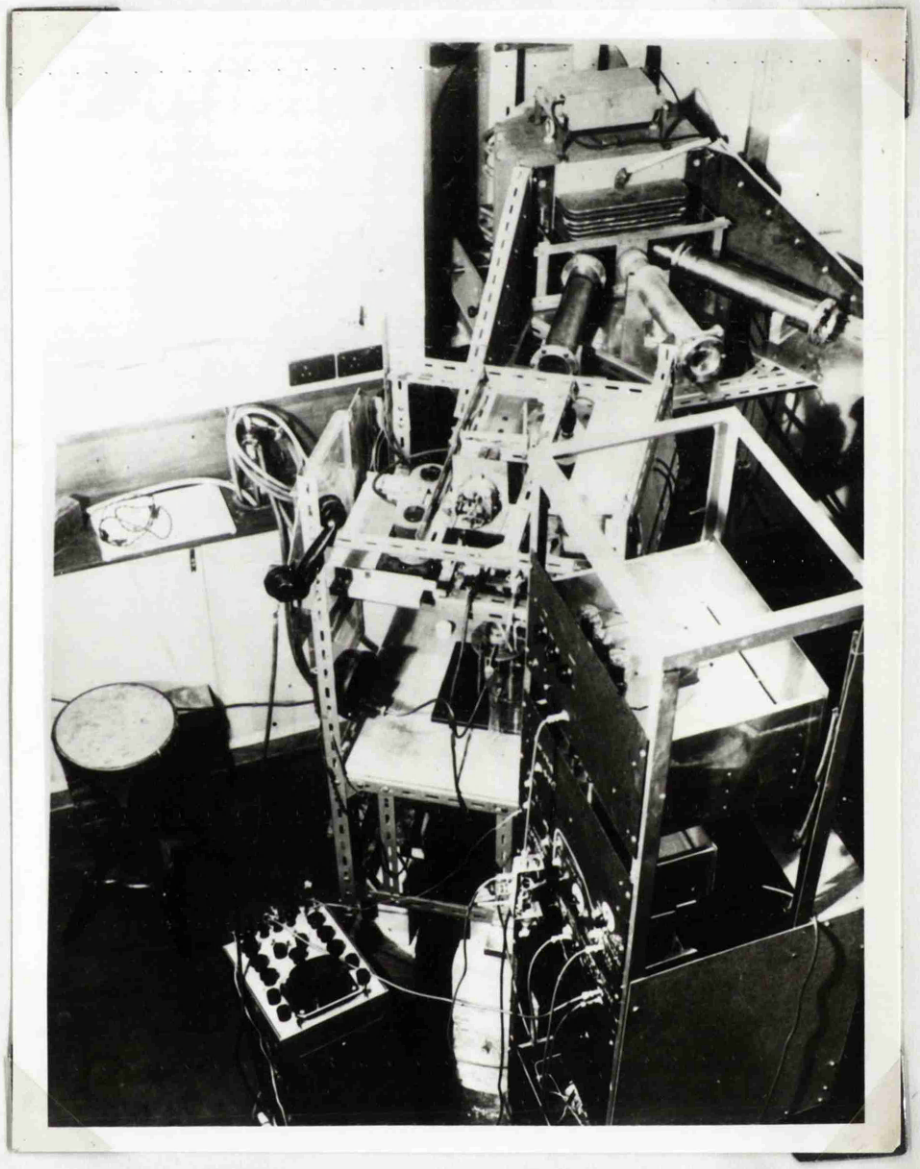

Plate (iii). The 20cc. chamber accepting electons from the pair spectrometer. The γ-ray beam emerges from the central tube.

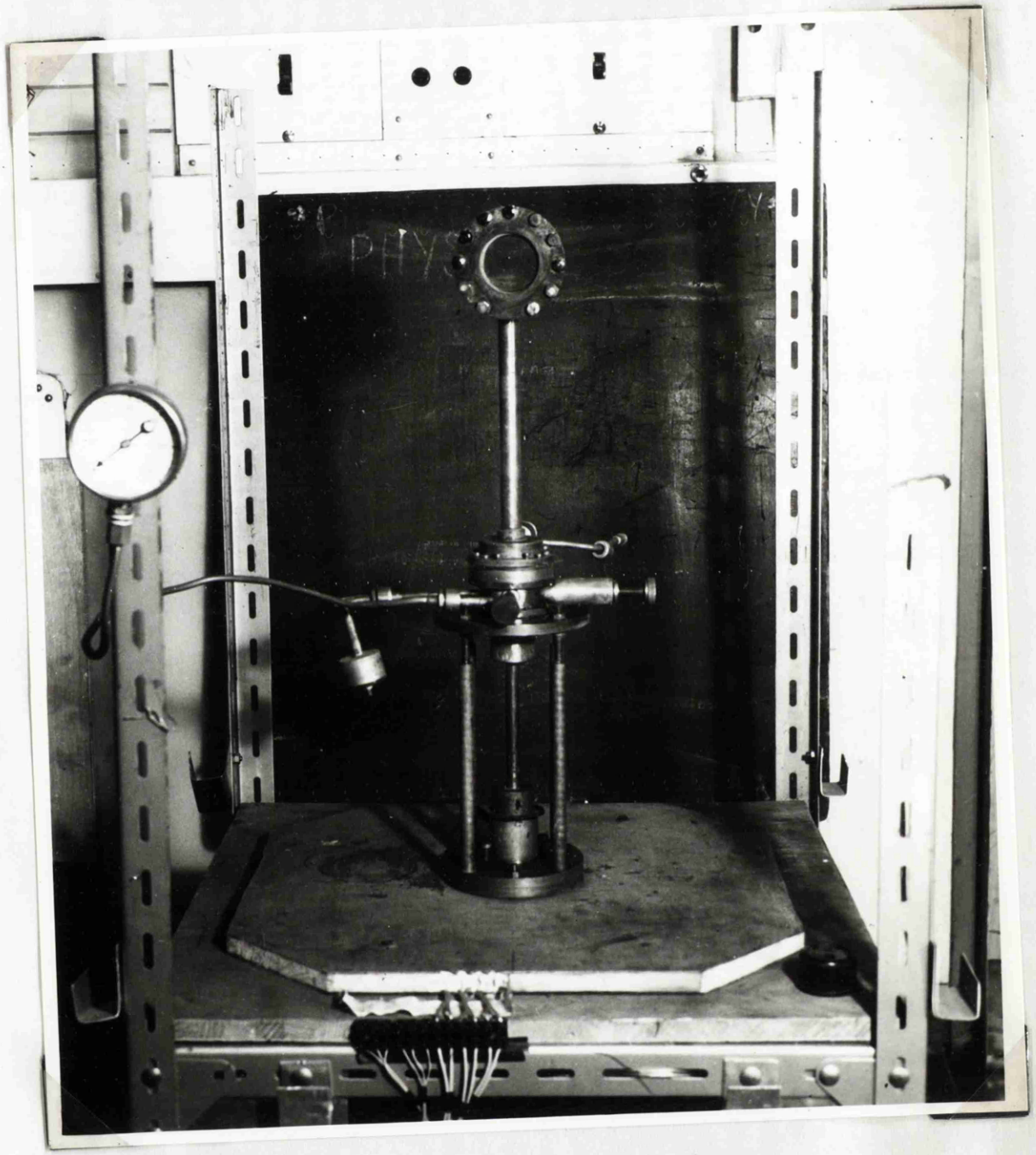

Plate (iv). The 100cc. 'dirty' chamber without the heating bath.

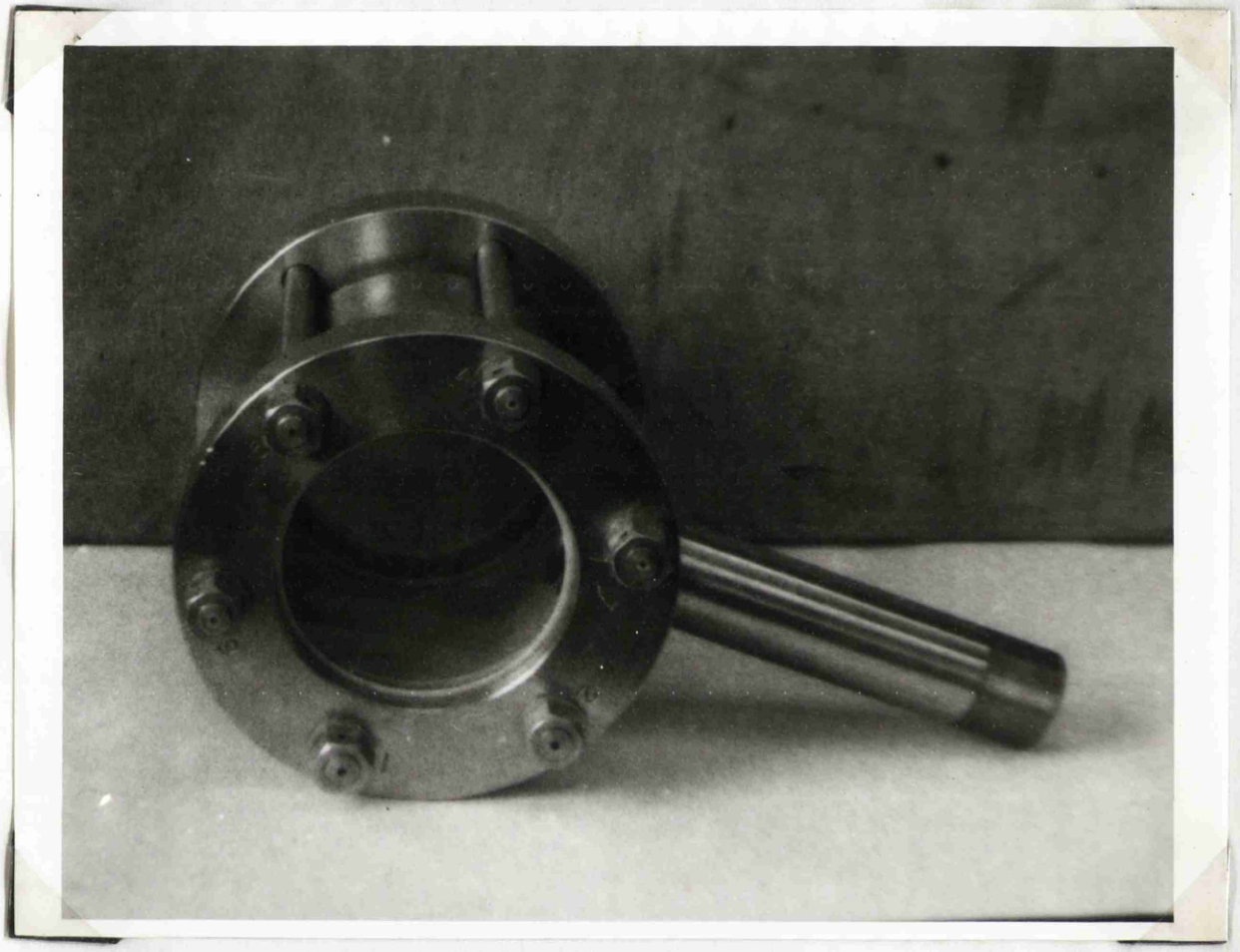

Plate (v). The 500cc. chamber detached from the expansion apparatus.

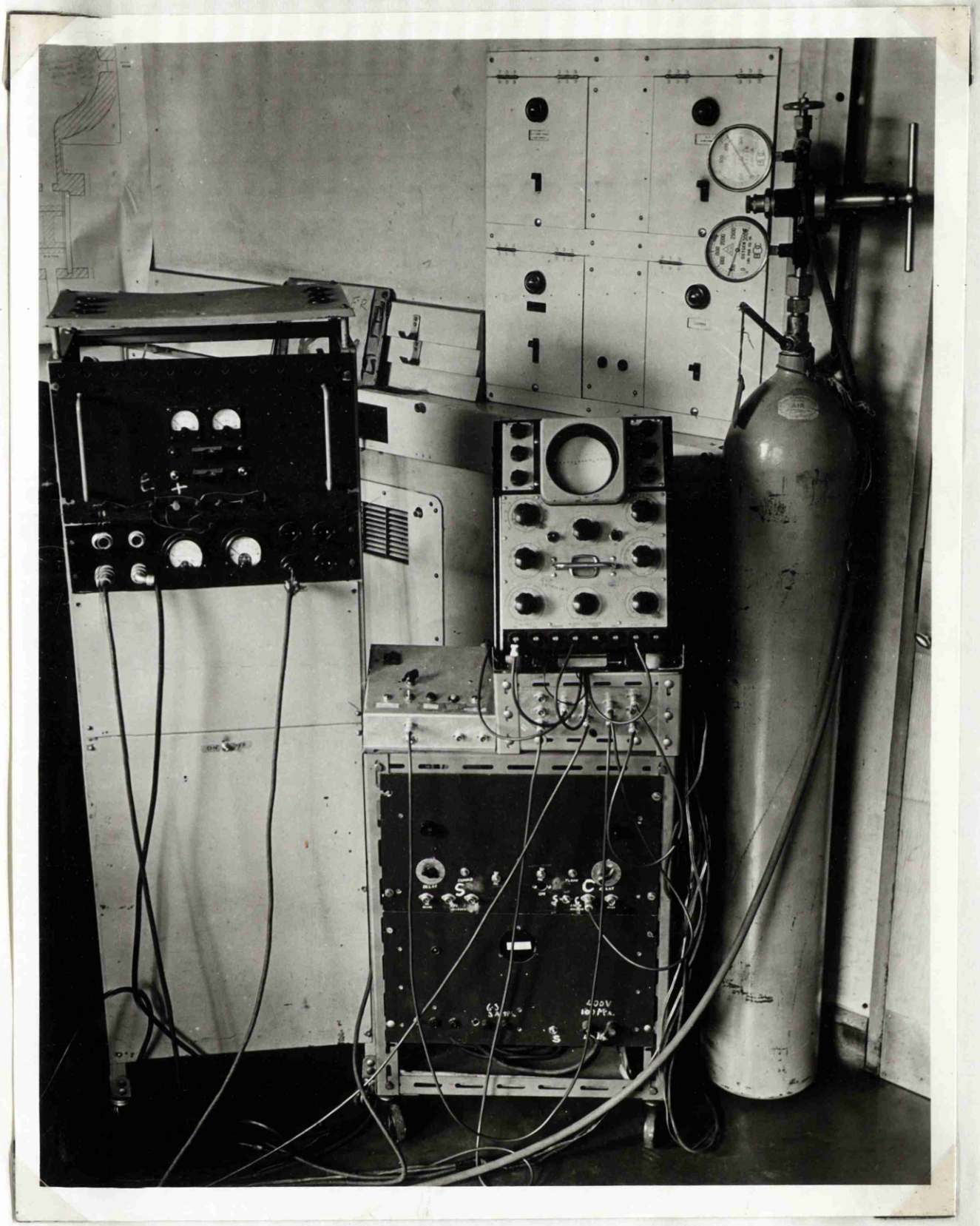

Plate (vi). The operating controls of the 5-litre chamber. These are situated remote from the chamber.

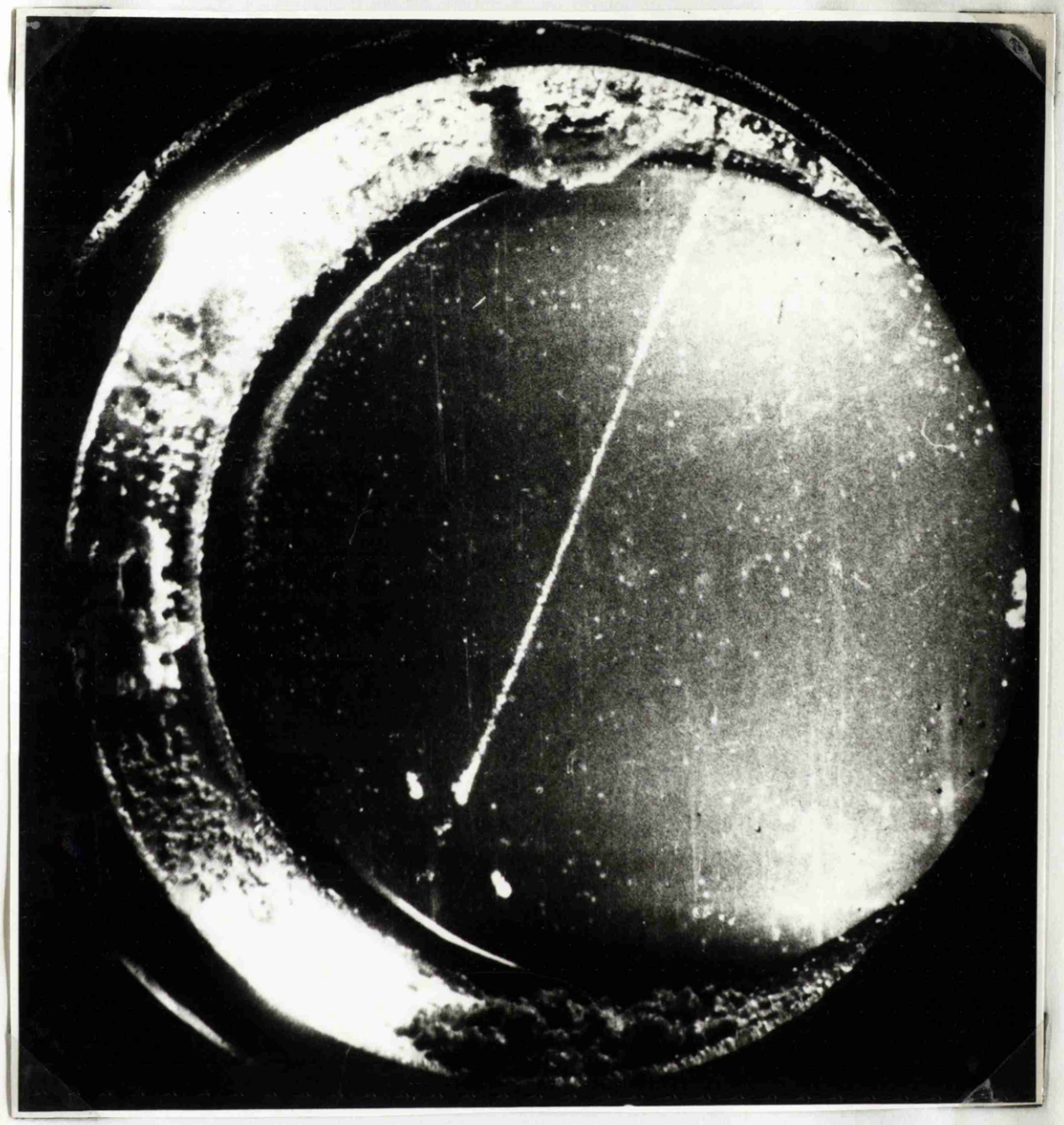

Plate (vii). A photograph taken at random which caught a cosmic ray at a late stage of bubble growth.

Plate (viii). A photoproduced π^+ - meson, decaying to μ^+ then e^+.

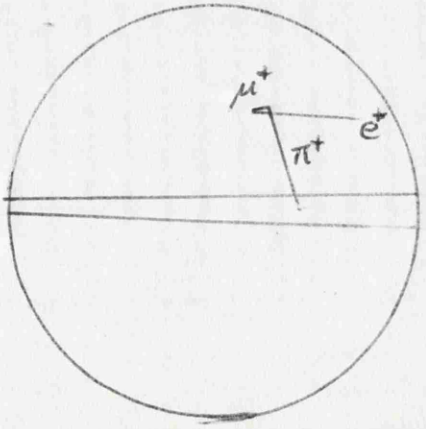

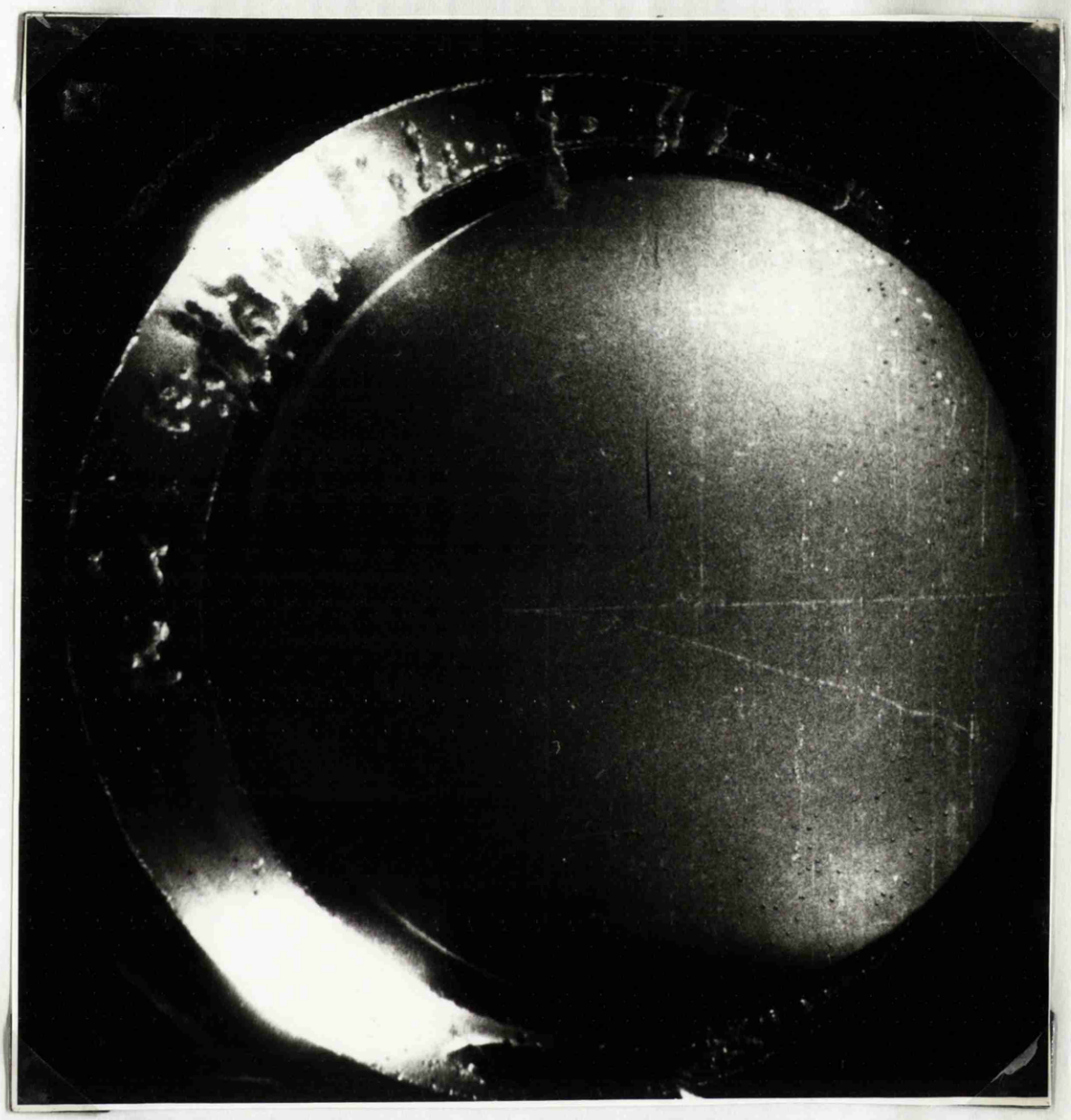

Plate (ix). An electron pair produced by a very low intensity Y-ray beam.